Inner Shell Electron Energy Loss Spectroscopy of Molecules of Interest for Proton Exchange Membrane Fuel Cells

Submitted by Robin Hayes
Supervisor: Dr. A.P. Hitchcock
Chemistry 4G09 Thesis
McMaster University
April 8, 2014

Table of Contents

List of Figures

List of Tables

List of Appendices

Abstract

The potential of proton exchange membrane (PEM) fuel cells to allow environmentally-friendly transportation is increasingly recognized, but a significant obstacle to the widespread use of PEM fuel cells is the susceptibility of their materials to degradation brought on by their operation. One tool that can help in detecting degradation-related changes is scanning transmission X-ray microscopy (STXM), a spectromicroscopy technique that is used to simultaneously visualize fuel cell materials and record their X-ray absorption spectra. Using STXM to characterize changes to fuel cell materials demands an understanding of the relationship between chemical structure and spectra. This project aims to further this understanding for one particular fuel cell material, perfluorosulfonic acid (PFSA). Using mainly inner shell electron energy loss spectroscopy (ISEELS) and some STXM, reference spectra of simple analogues of PFSA have been recorded at the S 2p and 2s, C 1s, O 1s and F 1s edges. Their peaks have been assigned to transitions from core to virtual orbitals, and the assignments are discussed with reference to comparable literature spectra and the results of *ab initio* calculations. The spectra give insight into the electronic changes imposed by structural modification to PFSA-like species. Differences in the spectra show that STXM spectra can be used to characterize changes in PFSA. Ways in which this can be done most efficiently are presented, with reference to particularly diagnostic trends that have been identified through the comparison of the reference spectra.

1. Introduction

1.1. Proton Exchange Membrane Fuel Cells

With papers and patents describing their use dating back to the 1970s, proton exchange membrane (PEM) fuel cells are not a new technology, but interest in them has undoubtedly spiked in recent years.[1, 2] As concern over emissions rates increases, finding an efficient means of powering environmentally-friendly transportation is becoming a more pressing goal. PEM fuel cells are increasingly regarded as a way to minimize emissions without having to sacrifice the convenience of personal motorized transportation.[3-5]

Proton exchange membrane (PEM) fuel cells produce electricity by the oxidation of hydrogen gas, which takes place in the membrane electrode assembly (MEA) on the catalyst-coated membrane.[6] The MEA consists of bipolar plates sandwiching a proton exchange membrane, as in **Figure 1**.[6] Opposite ends of the membrane are coated with carbon support and catalyst layers to give two electrodes.[7] Hydrogen is oxidized at the anode, yielding electrons and protons. The electrons pass through an external circuit and generate a current, while protons move through the PEM to the cathode. At the cathode, oxygen is reduced and combined with two protons to give water.[3-7]

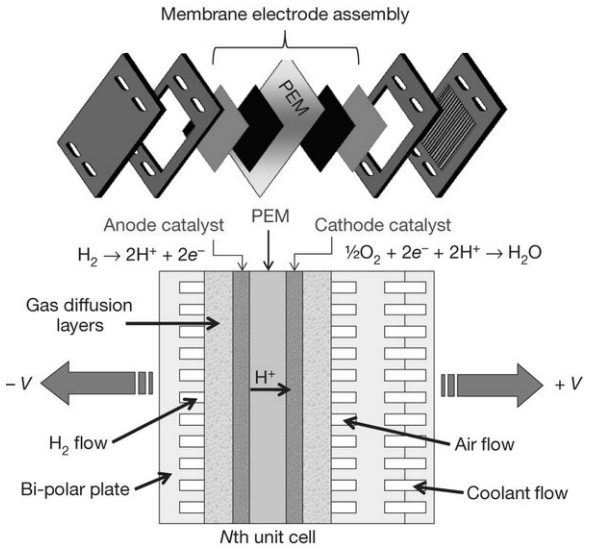

Figure 1. The membrane electrode assembly of a PEM fuel cell, consisting of bipolar plates sandwiching a proton exchange membrane coated on either side with catalyst layers.[6]

This process, which seems simple overall, places several requirements on the materials used in a catalyst-coated membrane. For instance, the carbon support coating the cathode must not corrode at high cell voltages, the membrane must conduct protons but prevent the passage of input gases and electrons, and the platinum catalyst particles on the electrodes must remain active and unagglomerated.[3,5,8-10]

The performance of the fuel cell is closely tied to the integrity of these materials, but the very conditions brought on by operation of the fuel cell can do significant damage to them. To be competitive with current automotive power systems, PEM fuel cells must remain efficient over 4000 driving hours and 30,000 startup and shutdown cycles.[5,9] Accelerated stress tests, which mimic many hours of operation in a short timespan, have shown that far fewer hours of use can be detrimental to fuel cell performance. Many degradation mechanisms and their results have been proposed. For one, corrosion of the cathode carbon support is a risk under low-fuel conditions. It can cause platinum catalyst particles to drift into the membrane and agglomerate, with further loss of platinum occurring at the high potentials of startup and shutdown, when Pt(0) catalyst particles are oxidized and dissolve into the membrane.[11] Both of these mechanisms create a platinum band, or region of high platinum density in the membrane, which reduces electrochemical surface area and decreases cell power.[8,9,11] Of most interest to this project is the potential for degradation of the perfluorosulfonic acid (PFSA) polymer used in the PEM, shown in **Figure 2**. Thermal degradation of the polymer can be caused by the exothermic combustion of H_2 and air that penetrates the PEM.[10] PFSA is also subject to chemical attack by peroxy radicals, which are formed in the platinum band from H_2O_2 generated by incomplete reduction of O_2 or gas crossover through the membrane.[5,7-10]

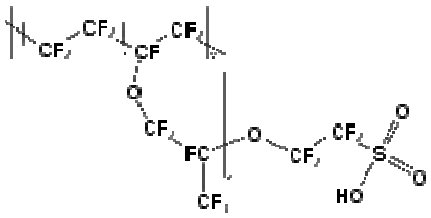

Figure 2. The perfluorosulfonic acid polymer used in the proton exchange membrane. The x, y and z subscripts indicate repeating units.

Since the performance of the fuel cell is so closely tied to the structure of all of these materials, the significant possibility for degradation is problematic. Although the ultimate goal may be said to be the development of materials that are more resistant to degradation, a more immediate challenge is to monitor changes in the structure or distribution of fuel cell materials. This can clarify the nature of degradation and the circumstances under which it takes place, and is crucial to the development of better fuel cells.

1.2. Scanning Transmission X-ray Microscopy (STXM) of Fuel Cell Materials

For this purpose, Scanning Transmission X-ray Microscopy (STXM) can be used. STXM is a spectromicroscopy technique. A sample is hit by a beam of X-rays, generated at a synchrotron radiation facility by the acceleration of electrons and sent along a beamline to the sample. The energies of the X-rays can be tuned by adjusting the grating angle of a monochromator on the beamline, and are scanned over a range that is typically absorbed by components of the sample. At each energy, the transmission of X-rays is recorded. It is converted to absorbance, or optical density (OD), showing how much of an absorbing material is present in the sample. Images of the sample at each energy and X-ray absorption spectra at each point in the sample are produced. Sequences of these images and spectra are called stacks. Stacks give information on the chemical identity of compounds in the sample, based on the spectra, and on their spatial location, with resolution down to 30 nm.[7]

This complementary information makes STXM well-suited to following changes in the structure and distribution of fuel cell materials after use. In one example, Bessarabov and Hitchcock[7] used STXM to investigate the formation of the platinum band in the membrane and its effects on the structures of nearby membrane components. STXM images and spectra were recorded on a cross-section of a fuel cell MEA before testing, and after subjecting the MEA to a simulated drive cycle. Images of the post-test sample recorded over an energy typically absorbed by carbon were fit to the spectra of four carbon-based membrane components. A Pt band was detected in the membrane as the constant of the fit. Images of the distribution and thickness of each component are shown in **Figure 3a**. C 1s spectra of the membrane near and far from the Pt band were then compared, shown in **Figure 3b**, and showed differences in spectral features. This STXM study confirmed that the presence of a Pt

band in the membrane is a direct result of operation of the fuel cell, and that the band affects membrane chemical structure.

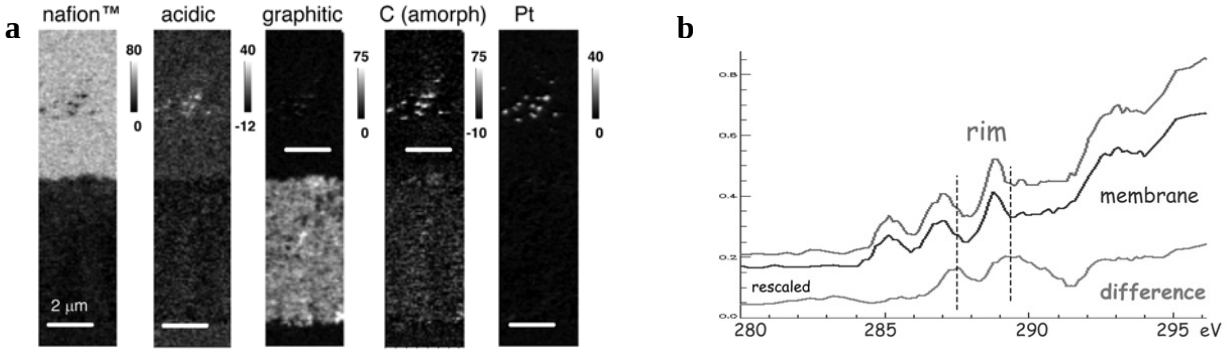

Figure 3. a) STXM images of an MEA cross-section, showing the distribution of four carbon components and the Pt band. **b)** A comparison of the C 1s spectra near ("rim") and far from ("membrane") the Pt band, showing that proximity to the Pt band affects spectral features.[7]

This case illustrates how the spatial resolution of STXM can be complemented by its spectroscopy component. It also indicates the importance of being able to interpret spectra to identify components and understand changes in their structure. If spectral features and chemical structure cannot be related, a change in the structure of membrane molecules near the Pt band may be detected, but the nature of this change will be uncertain. In this way, a lack of understanding of the relationship between spectral features and chemical structure limits the usefulness of STXM.

The STXM data presented in **Figure 4** show the difficulty that interpretation of X-ray absorption spectra presents routinely. This data was recorded on a cross-section of a cathode and membrane over the energy range absorbed by sulfur. The spectra show two sulfur components, distinguishable by their different peak energies and widths. One of these has spectral features that are typical of the sulfur compound typically found in fuel cells ("Expected S species"). The other one has features that do not match those of the expected compound ("Mystery S species"). Without knowledge of how sulfur spectroscopic differences relate to structure, or similar spectra to compare to, the identity of the second component is a mystery.

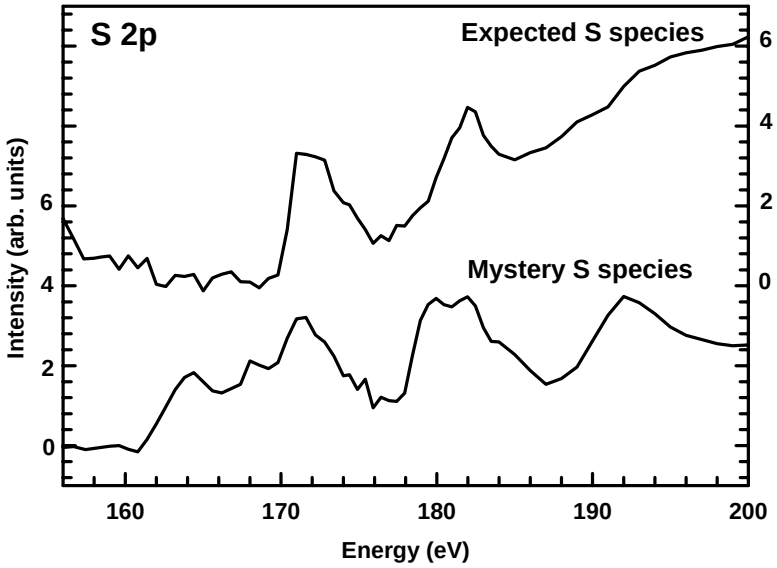

Figure 4. S 2p spectra recorded on a cross-section of a cathode and membrane, showing two different sulfur species. The identity of the sulfur species that gives the spectrum on the bottom is unknown.

1.3 The Role of ISEELS

This thesis project is an attempt to address these sorts of barriers to the effective use of STXM data. Using STXM to follow changes to fuel cell materials requires either an understanding of the relationship between spectra and chemical structure, or a library of reference spectra with which the spectrum of interest can be compared. With this in mind, this project focused on acquiring spectra of several pure gas-phase molecules using mainly inner shell electron energy loss spectroscopy (ISEELS), with a couple molecules run on STXM. The molecules used were chosen because they are simple analogues of the perfluorosulfonic acids (PFSA) polymers used in fuel cells, shown earlier in **Figure 2**. These polymers have a polytetrafluoroethylene (PTFE) backbone and pendant sulfonate heads, and are found in the membrane.[5,10] Protons can hop between the sulfonate heads of PFSA, giving the membrane its proton-conduction properties.[3] Because it has such a key role, monitoring changes in the structure and spatial location of PFSA during fuel cell use is desirable. This motivated the choice of reference molecules studied here, shown in **Figure 5** and referred to hereafter as “the sulfonate family” or “the five molecules studied” for brevity. The substrate on the single-bonded oxygen and fluorination of the methyl sidechain were varied between

reference molecules to reflect some changes that PFSA could be expected to undergo in a fuel cell. The aim was to gain some understanding of the electronic changes imposed by structural differences in sulfur compounds, and to highlight spectral fingerprints of these compounds that could be used to identify important changes in PFSA in a fuel cell.

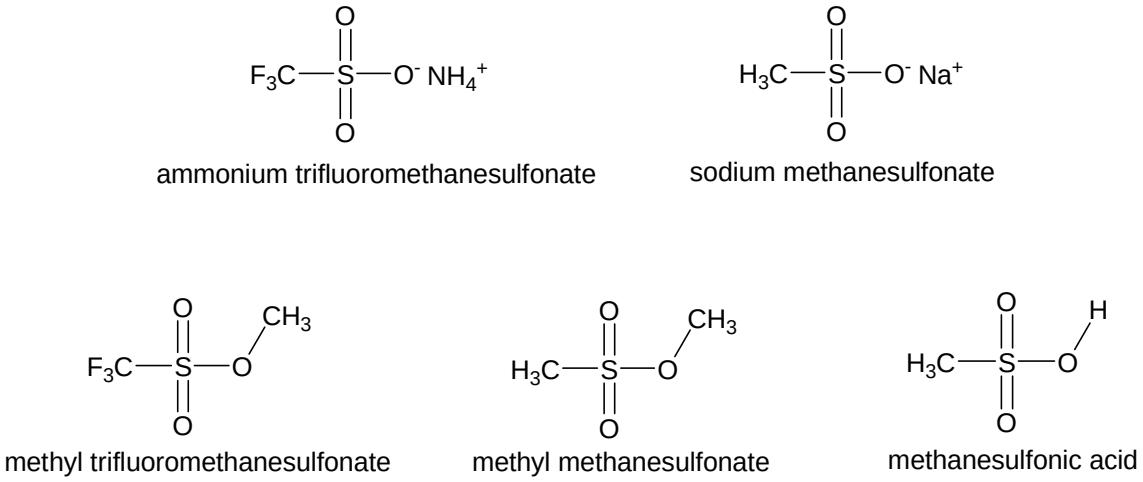

Figure 5. Sulfonate-related species whose spectra were measured.

ISEELS was the spectroscopic technique of choice for this project because it gives spectra that can be compared to those acquired on STXM, but allowed the compounds to be studied at McMaster. In STXM, a beam of photons is focused onto a sample. In ISEELS, electrons replace the photons, but conditions are used that mimic photoabsorption so that the spectra can be related to STXM spectra.

ISEELS requires that samples be in the gas phase, so that incoming electrons are scattered but not absorbed completely. The gaseous samples are held in a gas cell inside the spectrometer. When an electron (e^-) hits a target molecule (M) in the gas phase, it is scattered inelastically according to the following process, where E is energy and k is momentum:

$$\begin{array}{lcccc} e^- & + & M & \longrightarrow & M^* + e^- \\ E_0 & & & & E_n \quad E_1 \\ \underline{k_0} & & & & \underline{k_1} \end{array}$$

Under conditions of low momentum transfer ($\underline{k}_0$-$\underline{k}_1$ is small), only dipole-allowed transitions are permitted. The incident electron excites an electron from a localized core orbital, such as C 1s, to an unoccupied, virtual orbital, losing an amount of energy ($E_n=E_0-E_1$) that is equivalent to the transition energy in the process. The transition energy depends on the atomic core from which the electron is excited, as well as on the environment of that atom. Spectra therefore give information about the types of chemical environments found in a molecule, which can be used to elucidate its structure. The probability of particular transitions in a molecule is reflected by the intensity of peaks.[12]

2. Experimental

2.1. Sample Sources and Purities

Methyl methanesulfonate ($CH_3SO_3CH_3$), methyl trifluoromethanesulfonate ($CF_3SO_3CH_3$), methanesulfonic acid (CH_3SO_3H), ammonium trifluoromethanesulfonate ($NH_4CF_3SO_3$) and sodium methanesulfonate ($NaCH_3SO_3$) were obtained commercially from Sigma-Aldrich. The ammonium and sodium salts were crystalline solids, while the sulfonic acid and sulfonic acid esters were viscous liquids. The stated purities are 99.5% for methanesulfonic acid, 99% for methyl methanesulfonate and ammonium trifluoromethanesulfonate, and 98% for methyl trifluoromethanesulfonate and sodium methanesulfonate. They were used without further purification, except that afforded by distilling the samples into the spectrometer. The identity of methanesulfonic acid was confirmed by mass spectrometry on a sample derivatized to make the trimethylsilyl ester because the acid itself was too polar to detect. The mass spectrum is shown in Appendix 1. The molecular ion peak, at m/z=153.1, corresponds to the TMS (73.12 g/mol) ester of methanesulfonic acid (96.11 g/mol) minus an H (1.01 g/mol) and a CH_3 group (15.03 g/mol). In a headspace analysis, no other volatile components were detected. This confirmed that the sample was indeed methanesulfonic acid.

2.2. Inner Shell Electron Energy Loss Spectroscopy (ISEELS)

Inelastic electron scattering experiments were carried out on the liquid samples – methyl methanesulfonate, methyl trifluoromethanesulfonate and methanesulfonic acid – on

an electron spectrometer located at McMaster. The spectrometer, known as ISEELS, has been described in detail elsewhere,[12] but an overview of its most important features and functions is given here.

The schematic in **Figure 6** describes the journey made by an electron in ISEELS. The electron source is an electron gun with a barium strontium oxide emitting surface. Electrons pass from the gun into a scattering column, which is made up of plates and apertures that deflect and narrow the beam. The beam passes through a gas cell, into which the sample vapour is funneled. When no sample is being run, the entire inside of the instrument is held at a vacuum of around $3x10^{-7}$ torr by diffusion pumps. During experiments, a pressure gauge provides a way of checking if there is sufficient sample inside the instrument. Spectra are generally recorded at pressures in the range of $1 – 5x10^{-6}$ torr, but even pressures on the order of 10^{-7} torr can be sufficient.

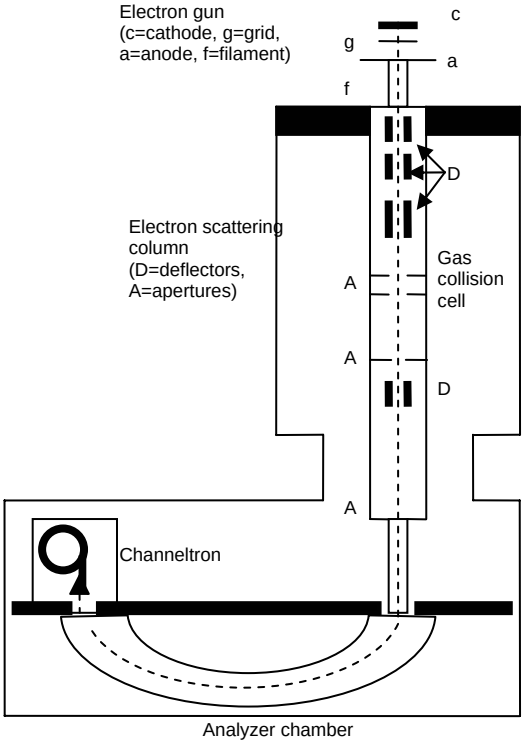

Figure 6. Schematic of the inside of the ISEELS spectrometer.

The spectrometer was operated under a set of conditions that favour electric dipole-allowed transitions by minimizing momentum transfer. A 2^0 scattering angle and a 2.5 keV final electron energy were imposed.

After interacting with the sample, electrons enter the analyzer. The analyzer is operated at 40 eV pass energy. Only the electrons with that energy after inelastic scattering and deceleration can go through a 1 mm exit aperture and be received by a channeltron. The channeltron detects the number of electrons that have lost a certain amount of energy to the sample, which is a measure of the likelihood with which electrons in the gas molecules will make a transition of that energy.

The spectrometer has three entrance ports for samples, which are indicated in **Figure 7**. The choice of a port depends on the volatility of the sample. The sulfonic acid esters were sufficiently volatile that a vial containing approximately two millilitres of liquid could be attached to sample port **a**. When the samples were gently heated with heating tape attached to a VARIAC, vapour was pulled through copper tubing into the gas cell inside the spectrometer. The pressure inside the spectrometer can be controlled with leak valves. The less-volatile sulfonic acid had to be placed inside the spectrometer via port **c**, in a vial with a tygon tube leading directly into the gas cell.

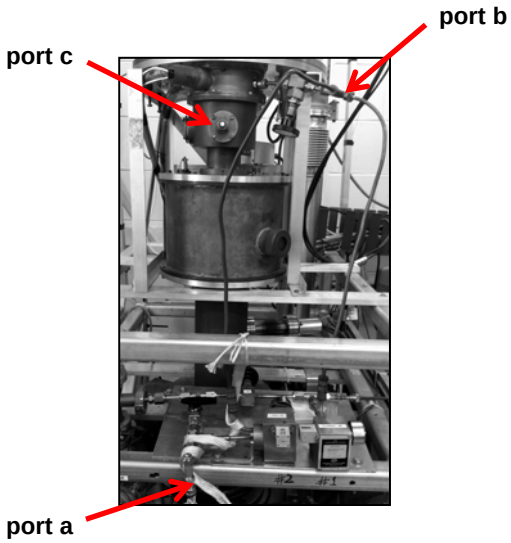

Figure 7. The ISEELS instrument, with the three sample ports indicated. Port **a** is used for the most volatile species, port **b** for less volatile species, and port **c** for species that are the least volatile.

Multiple spectra were recorded each time a sample was introduced, to check reproducibility of the spectra. This was done to ensure that any volatile impurities had been distilled off and samples were not decomposing.

The S 2p and 2s, C 1s and O 1s spectra of all liquid samples, and the F 1s spectrum of methyl trifluoromethanesulfonate, were recorded. Long-range spectra were acquired at a beam current of ~20 μA, for a resolution of ~0.8 eV FWHM. High-resolution spectra were recorded only over regions of particular interest for the S 2p, C 1s and O 1s edges at a beam current of ~3 μA, for a resolution of ~0.5 eV FWHM. The energy-loss scale was calibrated by simultaneously recording spectra of the samples and CO_2 or O_2, then referencing to the known energies of the C 1s→π* and O 1s→π* transitions of CO_2 (C 1s: 290.74(4) eV; O 1s: 534.4(2) eV) or the O 1s→π* transition of O_2 (530.8(1) eV).[13,14]

Multiple spectra recorded at each edge were added together, with the high-resolution spectra used for areas with fine spectral features. Background subtraction of a curve fit to the pre-edge signal was used to eliminate the underlying valence-shell and core excitation continua. To allow comparison on a per-atom basis, the spectra were converted to absolute oscillator strength scales by applying a kinematic correction to the spectra, then normalizing to calculated atomic continuum photoionization oscillator strengths.

2.3. Scanning Transmission X-Ray Microscopy (STXM)

Sodium methanesulfonate and ammonium trifluoromethanesulfonate are solids that could not be run on ISEELS because they are not sufficiently volatile. These samples were taken to two synchrotron facilities, the Canadian Light Source (CLS) in Saskatoon and the Advanced Light Source (ALS) in Berkeley, to use the bending magnet scanning transmission microscope at these facilities. A couple milligrams of the samples were dissolved in about 5 mL of ethanol. The concentration of the solution was tested by spotting it onto a microscope slide and looking at it under an optical microscope, and the concentration was adjusted so that particles of the solid were dispersed thinly. A small drop (~0.5 μL) of this solution was dropped onto an X-ray-transparent silicon nitride window. When it dried, it formed a thin film over the window. A region of the film that was sufficiently thin to give an optical density of about 1 (~100 nm) was used for STXM measurements.

S 2p, C 1s and O 1s spectra were recorded for both samples. For sodium methanesulfonate, spectra were also recorded at the Na 1s edge. For ammonium trifluoromethanesulfonate, the F 1s and N 1s edges were measured as well. To allow for a comparison with the ISEELS spectra, the S 2p, C 1s, O 1s and F 1s STXM spectra reported here have been scaled so that the pre-edge and post-edge intensities match those of the most similar ISEELS spectrum. In Appendix 2, the spectra normalized to their OD1 values (optical density per nm) by matching to calculated spectra for each edge are presented.

To allow for a comparison of STXM and ISEELS results, a sample of methyl trifluoromethanesulfonate was also run on STXM. A wet cell was prepared by using epoxy to glue two silicon nitride windows together, and pipetting a small amount (~0.5 μL) of methyl trifluoromethanesulfonate into the cell, then sealing the edges with epoxy. The compound was found to dissolve the epoxy slightly, but contamination was not so bad as to prevent acquisition of methyl trifluoromethanesulfonate spectra. By the time the sample was run on STXM, the compound seemed to have formed a solid film on the cell windows rather than existing as a liquid, but a region of appropriate optical density was found and spectra were recorded in this area.

In all cases, images of the regions of interest were recorded before and after acquiring X-ray absorption spectra, to check for changes to the sample. Methods including defocusing of the beam and rapid scanning of lines were used to minimize radiation damage to the materials. In cases were radiation damage was apparent, new areas of the sample were used for each edge. This was especially important for ammonium trifluoromethanesulfonate, which showed significant changes in morphology especially at the F 1s edge after spectra were recorded.

2.4. Ab Initio Calculations

To assist in assigning spectral features, calculations of the inner shell spectra of methanesulfonic acid were performed using Kosugi's GSCF3 package (Gaussian Self-Consistent Field version 3).[15] GSCF3 is an *ab initio* method that is specialized for inner shell excitation and ionization calculations. GSCF3 is based on the Improved Virtual Orbital approximation, which takes into account the core hole in the Hartree-Fock approach. To use these calculations, the user must first input the geometry of the molecule. The geometry of

methanesulfonic acid was optimized using SPARTAN at the 6-31G* level. GSCF3 calculations then proceed in three steps. In the first, the ground state energy of a user-specified atom is calculated, and the atomic orbital that will lose an electron is determined. Next the core hole is placed on the specified atom, and the energy of the new state is found. The difference in energy between the core ionized and ground states of the atom give its ionization potential (IP), with an accuracy of 1 eV. Finally, the third step calculates the energy of the excited state of the atom. This step gives core excitation term values, which specify the energy of a transition, and oscillator strengths, which give transition intensities. The term values and oscillator strengths are used to simulate inner shell spectra. This is repeated for each distinct atom in the molecule, and the spectra of all the atoms of one type are summed together to give a predicted spectrum at that edge. The energies of transitions in the calculated spectra are usually overestimated, so calculated spectra are shifted to match experimental spectra. Based on the GSCF3 results, molecular orbital images can also be generated to show the nature of the orbitals to which excitations take place.

Huzinaga-type basis sets must be specified for each atom.[16] In the input files used for methanesulfonic acid, the basis sets and contraction schemes for the core excited atoms were HTS6X (41121/2111) for carbon and oxygen and HTS3X (533/53) for sulfur. For non-excited atoms, HTS4X (53/4) for carbon and oxygen, HTS0X (333/33) for sulfur and HTS3X (6) for hydrogen were used.

Spectra were calculated for methanesulfonic acid at the S 2p, C 1s and O 1s edges. The spectra are shown in Appendix 3, plotted below the experimental methanesulfonic acid spectra for comparison. For the first several discrete peaks of each spectrum, images of orbitals to which the transitions take place are shown, and the peak energies, oscillator strengths and assignments are given in a table.

3. Results and Discussion

The significant spectral features of each molecule at each edge have been assigned, and in the following sections the assignments are justified with reference to literature spectra of comparable molecules and the results of GSCF3 calculations. Because the project was motivated by the goal of identifying important changes in PFSA spectroscopically, a discussion of the contribution that each edge can make to this goal is also presented.

3.1. Sulfur 2p and 2s Edges

3.1.1. Peak Assignments

The S 2p and 2s spectra of the five molecules studied are shown in **Figure 8**, and **Table 1** gives peak energies and assignments. The first distinct peak, around 170 eV in each molecule, is actually made up of three peaks, as the enlarged subregion of three spectra in **Figure 9** shows. This distinctive triplet shape is seen in the ISEELS spectra of other sulfur-containing molecules and happens because spin-orbit coupling splits the S 2p orbitals into S $2p_{3/2}$ and $2p_{1/2}$ orbitals.[17-21] The features of the triplet peaks have been assigned in agreement with the reported features of DMSO, with transitions from $2p_{3/2}$ orbitals showing up at slightly lower energy than transitions from $2p_{1/2}$ orbitals, and transitions from both orbitals terminating at σ*(S-O) and σ*(S-C) molecular orbitals, and 4s and 4p Rydberg states.[19] In Rydberg states, excited electrons are held in a diffuse orbitals that can be characterized by a principal quantum number higher than that of the ground state, whose energies follow the Rydberg series for hydrogen and converge on the ionization potential of the atom.[22] These assignments are supported by reported thiolane and methanethiol transitions, which are to σ*(S-C) and Rydberg orbitals.[20,21] The transition to the 4p Rydberg state is expected to be weak because of the selection rule that requires that the orbital angular momentum quantum number change by one for dipole-allowed transitions.

The methanesulfonic acid GSCF3 calculations produced mainly orbitals of Rydberg character, which further supports the assignments. In order to line up the calculated and experimental spectra, the energy scale of the calculated sulfur spectrum had to be shifted by close to 15 eV, as opposed to the usual 1-3 eV shift needed. This is because the calculated IP of sulfur in methanesulfonic acid is 186.878 eV, while similar sulfur species have IPs around 173-174 eV.[17-19] Running the calculations with different basis sets and contraction schemes reported in the literature[23,24] had a negligible effect on the IP. As such, although the predicted excitations are in agreement with the experimental results and seem valid, attempts should be made to correct the energy scale, perhaps by adding compact functions on sulfur as recommended in one paper to account for contraction of the sulfur atom upon creation of the core hole.[23]

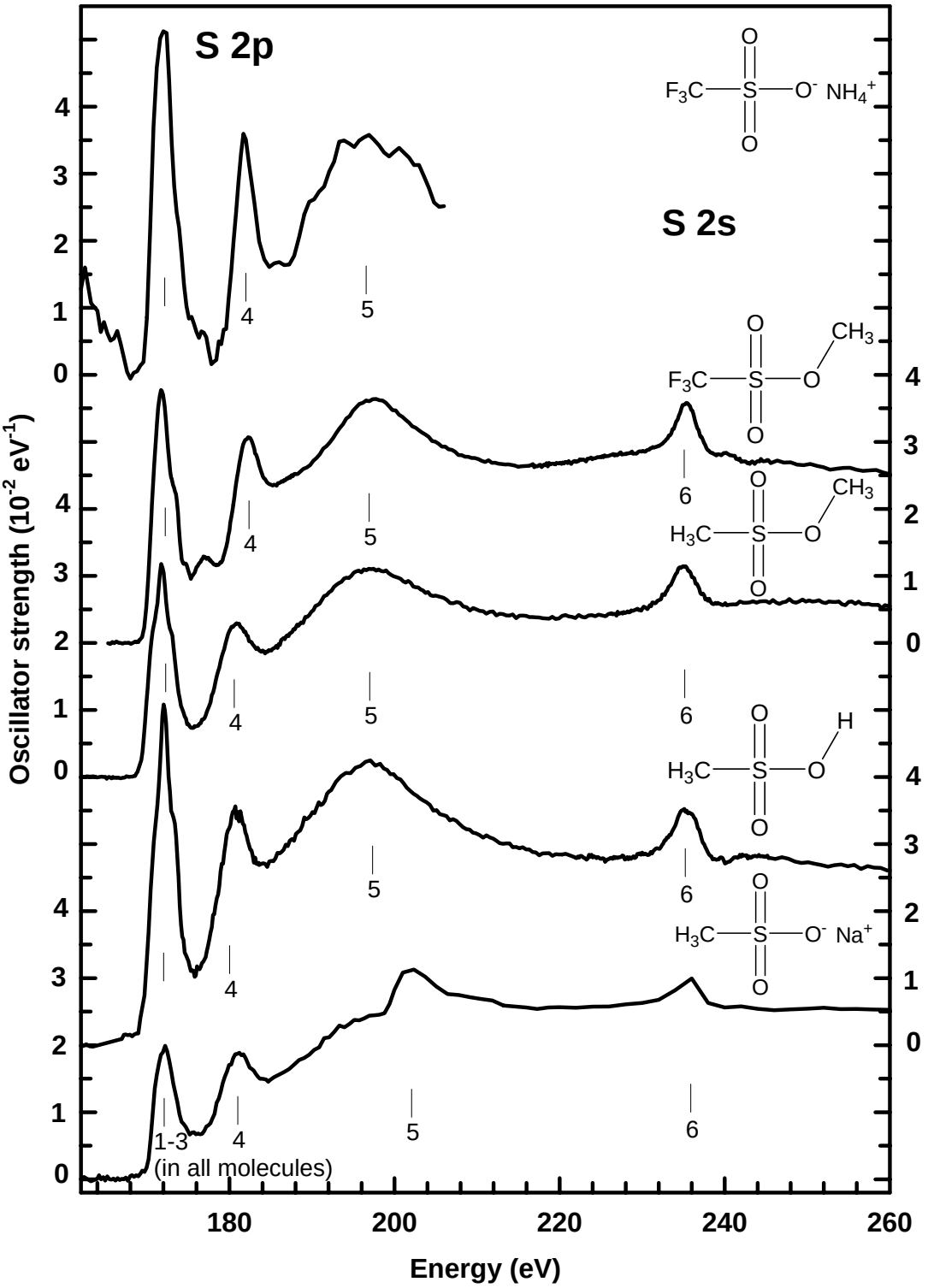

Figure 8. S 2p spectra of the species recorded.

Molecule	Feature	Energy loss (eV)	Assignment
Ammonium trifluoromethanesulfonate	1	172.03	$2p_{3/2},2p_{1/2}\rightarrow\sigma^*$(S-O), σ^*(S-C), 4s, 4p
	2	181.83	$2p\rightarrow3d(t_{2g})$ shape resonance
Methyl trifluoromethanesulfonate	1	171.75	$2p_{3/2}\rightarrow\sigma^*$(S-O), σ^*(S-C)
	2	173.50	$2p_{1/2}\rightarrow\sigma^*$(S-O), σ^*(S-C), $2p_{3/2}\rightarrow4s$
	3	174.73	$2p_{3/2}\rightarrow4p$, $2p_{1/2}\rightarrow4s$
	4	177.13	$2p_{1/2}\rightarrow4p$
	5	182.3	$2p\rightarrow3d(t_{2g})$ shape resonance
	6	197.63	$2p\rightarrow3d(e_g)$ shape resonance
	7	235.45	$2s\rightarrow\sigma^*$(S-C)
Methyl methanesulfonate	1	170.68	$2p_{3/2}\rightarrow\sigma^*$(S-O), σ^*(S-C)
	2	171.76	$2p_{1/2}\rightarrow\sigma^*$(S-O), σ^*(S-C), $2p_{3/2}\rightarrow4s$
	3	173.07	$2p_{3/2}\rightarrow4p$, $2p_{1/2}\rightarrow4s$
	4	180.89	$2p\rightarrow3d(t_{2g})$ shape resonance
	5	197.28	$2p\rightarrow3d(e_g)$ shape resonance
	6	234.98	$2s\rightarrow\sigma^*$(S-C)
Sodium methanesulfonate	1	172.22	$2p_{3/2},2p_{1/2}\rightarrow\sigma^*$(S-O), σ^*(S-C), 4s, 4p
	2	181.21	$2p\rightarrow3d(t_{2g})$ shape resonance
	3	202.35	$2p\rightarrow3d(e_g)$ shape resonance
	4	235.98	$2s\rightarrow\sigma^*$(S-C)
Methanesulfonic acid	1	170.88	$2p_{3/2}\rightarrow\sigma^*$(S-O), σ^*(S-C)
	2	172.02	$2p_{1/2}\rightarrow\sigma^*$(S-O), σ^*(S-C), $2p_{3/2}\rightarrow4s$
	3	173.38	$2p_{3/2}\rightarrow4p$, $2p_{1/2}\rightarrow4s$
	4	180.97	$2p\rightarrow3d(t_{2g})$ shape resonance
	5	196.97	$2p\rightarrow3d(e_g)$ shape resonance
	6	235.33	$2s\rightarrow\sigma^*$(S-C)

Table 1. Peak energies and assignments for the S 2p and 2s spectra of the species recorded.

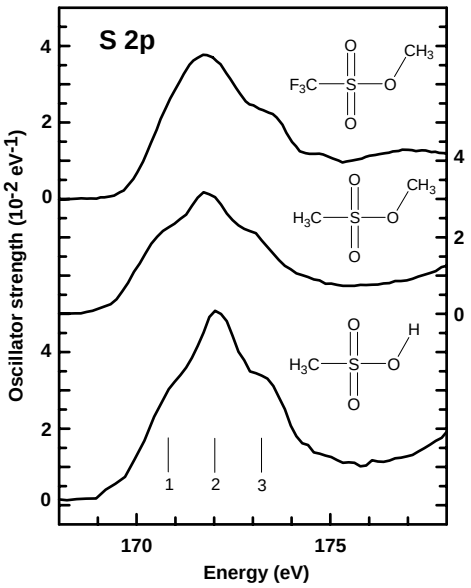

Figure 9. Enlarged region of the S 2p spectra of three of the sulfonates studied, showing the triplet shape of the first peak.

Above ~180 eV the peaks become broader. A similar pattern is observed in the photoabsorption spectrum of SO_2-containing poly(butene-1 sulfone) and the ISEELS spectra of SO_2, DMSO and thiolane, where the two highest-energy S 2p peaks are assigned to S 2p→3d shape resonances.[18-20,25] Shape resonances are caused by the trapping of an electron between centrifugal potential barriers, which arise due to the electrostatic forces of surrounding ligands.[26] In the case of many sulfur molecules, an electron excited to a 3d orbital becomes trapped in the well caused these barriers. The 3d orbitals are split into two e_g (higher energy) and three t_{2g} (lower energy) orbitals by the field generated by the sulfur ligands, and when the barrier is large, as is the case in molecules with electronegative ligands, the wavefunctions of electrons these orbitals have discrete energies.[19] Transitions to such orbitals are visible as clear, if broad, peaks. For the sulfonates, the three oxygens bonded to sulfur are sufficiently electronegative to produce obvious peaks corresponding to transitions to these 3d orbitals at ~180 eV and ~200 eV.

The feature that appears above 230 eV in the spectra of these molecules is assigned to a transition from a 2s orbital. In the spectrum of thiolane, the dominant feature is attributed to a transition to a σ*(S-C) orbital.[20] That assignment has been borrowed here.

3.1.2. Discussion of Important Results from the S 2p Edge

As discussed earlier, PFSA can undergo a range of changes over the lifetime of a fuel cell that will affect a fuel cell's performance. An example of a structural difference worth monitoring is the degree of fluorination of the PTFE backbone. Although the backbone of PFSA is supposed to be completely fluorinated, it has been reported that errors in the synthesis of PTFE can give some CH bonds.[5] It is not known conclusively whether this affects fuel cell performance, but being able to identify such faulty PTFE could answer this question. Direct changes to the sulfonate groups have also been reported, brought on by peroxide radicals.[5,10] These could interfere with the proton conduction abilities of PFSA.[5,10]

The S 2p spectra of these molecules show no distinctively different features, but a trend in the energy of the 3d(t_{2g}) peak is observed. Fluorination of the carbon attached directly to the sulfur shifts the peak to higher energy by about one eV. This is probably because fluorination pulls electron density away from the sulfur atom, exposing the sulfur

atomic orbitals to the nuclear charge. The sulfur 2p orbitals are lowered in energy more than the diffuse 3d orbitals, resulting in a larger energy gap between the two sets of orbitals.

The molecules studied here are all S(IV) compounds. Changes to the oxidation state of sulfur, which could occur in a fuel cell by structural modifications or exposure to the anode and cathode potentials, could also have an impact on spectral features.[11] Because of this, the spectra recorded on these sulfur(IV) molecules were compared to spectra reported by others of sulfur compounds similar in structure but in different oxidation states: SO_2(0),[18] DMSO(II),[19] and SO_4^{2-}(VI).[27] The spectra of these sulfur compounds are shown in **Figure 10.** Methyl methanesulfonate has been chosen to represent the S(IV) compounds because all of their spectra are nearly identical.

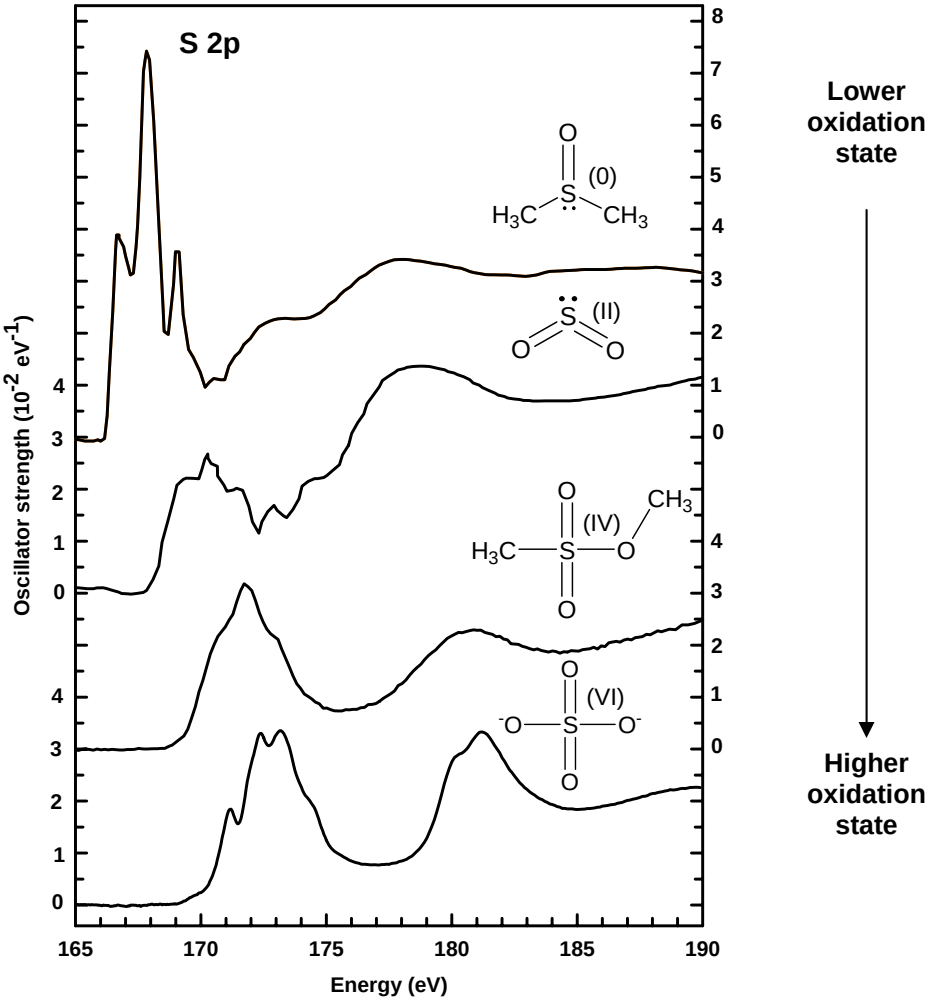

Figure 10. S 2p spectra of species in different oxidation states.

Another trend becomes evident through this comparison. The lowest-energy peak, which appears at 170.68 eV in methyl methanesulfonate, moves to higher energy as oxidation state is increased. This is attributed to the increased exposure of the S 2p orbital to the nuclear charge in higher oxidation states, which lowers the energy of the S 2p orbital more than those of the orbitals in which excitation terminates.

Spectra of sulfur compounds recorded on STXM could be matched to these two trends to determine the oxidation state and degree of fluorination near the sulfur atom. The effectiveness of this method was tested on the S 2p spectra introduced earlier, which were recorded on a cross-section of a fuel cell and showed an unidentifiable sulfur compound. The reference spectra and fuel cell spectra are all shown in **Figure 11**.

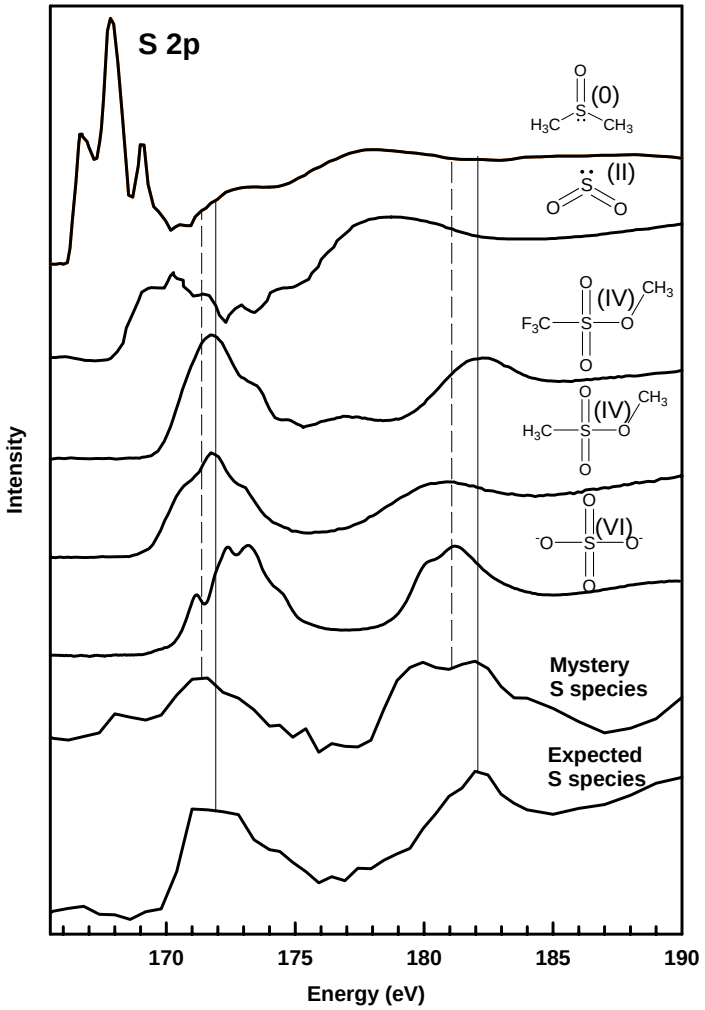

Figure 11. Reference spectra compared to STXM spectra of an expected S species (solid line comparison) and an unidentified S species (dashed line comparison).

The features of the expected sulfur species agree very well with the features of methyl trifluoromethanesulfonate. Since the only sulfur species expected in fuel cells is PFSA, this confirms that methyl trifluoromethanesulfonate is a good reference for PFSA. In the spectrum of the unidentified sulfur species, the shift of the 3d(t_{2g}) peak to lower energy suggests that the mystery sulfur species has a sulfur atom in close proximity to C-H rather than C-F bonds, and the shift of the lowest-energy peak indicates that this species might be in a lower oxidation state than PFSA. The poor quality of the STXM data prevents this comparison from being conclusive, but it does indicate that these reference spectra can be helpful in diagnosing modifications to PFSA.

3.2. Carbon 1s Edge

3.2.1 Peak Assignments

The C 1s spectra of the five molecules studied are shown in **Figure 12**, and **Table 2** gives peak energies and assignments. The two highest-energy peaks in the spectra of the fluorinated molecules are typical of molecules with C-F bonds. An ISEELS study by Ishii *et al.*[28] identified similar peaks in the region of ~295 eV and ~298 eV for every three-to-six-carbon perfluoro-*n*-alkane and assigned them to transitions to σ*(C-F) orbitals. It might be expected that only one peak to such an antibonding orbital would appear, since the C-F bonds in the CF_3 group of the sulfonates are identical. Ishii *et al.* hypothesized that the peaks differ in energy because the lower-energy transition is to a σ*(C-F) orbital of e symmetry within the C_{3V} point group of the CF_3 group, while the higher-energy transition is to a σ*(C-F) orbital of a_1 symmetry which, based on *ab initio* calculations, sits about 2.92 eV higher in energy. This also explains the higher intensity of the lower-energy peak, since the $\sigma^*(C\text{-}F)_e$ orbital is doubly-degenerate while the $\sigma^*(C\text{-}F)_{a1}$ orbital is nondegenerate.[28] The peaks in the spectra of the fluorinated molecules studied here show similar energy and intensity differences, so they have been assigned to the same transitions.

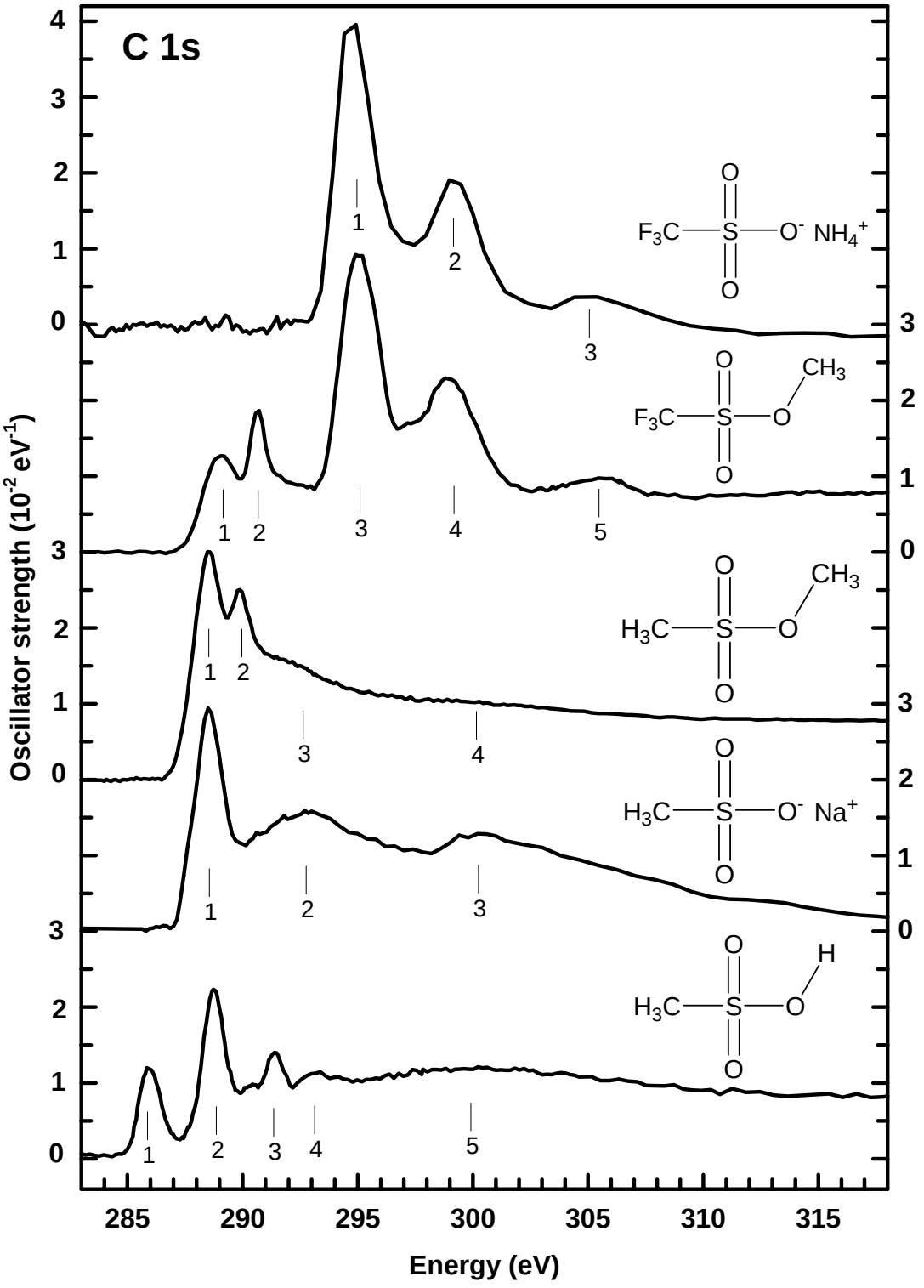

Figure 12. C 1s spectra of the species recorded.

Molecule	Feature	Energy loss (eV)	Assignment (from C 1s)
Ammonium trifluoromethanesulfonate	1	294.89	$\sigma^*(C\text{-}F)_e$
	2	299.02	$\sigma^*(C\text{-}F)_{a1}$
	3	304.95	shape resonance
Methyl trifluoromethanesulfonate	1	289.10	$3s/\sigma^*(C\text{-}H)_{C\text{-}O}$, $\sigma^*(C\text{-}S)$
	2	290.69	$3p/\sigma^*(C\text{-}H)_{C\text{-}O}$
	3	295	$\sigma^*(C\text{-}F)_e$
	4	298.88	$\sigma^*(C\text{-}F)_{a1}$
	5	305.71	shape resonance
Methyl methanesulfonate	1	288.57	$3s/\sigma^*(C\text{-}H)_{C\text{-}O}$, $3p/\sigma^*(C\text{-}H)_{C\text{-}S}$, $\sigma^*(C\text{-}S)$
	2	289.85	$3p/\sigma^*(C\text{-}H)_{C\text{-}O}$
	3	292.27	$\sigma^*(C\text{-}O)$
	4	299.93	shape resonance
Sodium methanesulfonate	1	288.52	$3p/\sigma^*(C\text{-}H)_{C\text{-}S}$, $\sigma^*(C\text{-}S)$
	2	292.89	$\sigma^*(C\text{-}O)$
	3	300.35	shape resonance
Methanesulfonic acid	1	285.96	$\sigma^*(C\text{-}S)$
	2	288.78	$3p/\sigma^*(C\text{-}H)_{C\text{-}S}$
	3	290.45	?
	4	293.37	?
	5	300.46	shape resonance

Table 2. Peak energies and assignments for the C 1s spectra of the species recorded.

In the spectrum of methyl trifluoromethanesulfonate, the peaks seen in ammonium trifluoromethanesulfonate are preserved nearly perfectly, but two new peaks appear several eV lower, suggesting that they are caused by transitions in the CH_3 group. In the spectra of alcohols such as methanol and propanol, peaks at similar energies are assigned to mixed Rydberg/molecular orbital transitions of $3s/\sigma^*(C\text{-}H)$ and $3p/\sigma^*(C\text{-}H)$ character.[29] The same assignments are used for alkanes, with the $3s/\sigma^*(C\text{-}H)$ transition showing up only as a lower-energy shoulder on the $3p/\sigma^*(C\text{-}H)$ peak.[28] These assignments have therefore been used here.

Sodium methanesulfonate shows only one broad peak in the CH_3 region. This peak is attributed to a $3p/\sigma^*(C\text{-}H)$ transition, mainly by analogy to the spectra of alkanes. The $3s/\sigma^*(C\text{-}H)$ transition, which is only a shoulder in the spectrum of alkanes, is probably lost in this main $3p/\sigma^*(C\text{-}H)$ peak. Since the electronegativity of sulfur is much closer to that of carbon than oxygen, it seems reasonable that the features of a CH_3 group bonded to sulfur would more closely resemble those of CH_3 groups in alkanes than alcohols.

The situation becomes slightly more complicated for methyl methanesulfonate because of its two CH_3 groups. The methyl methanesulfonate peaks are at similar energies to

the CH_3 peaks in methyl trifluoromethanesulfonate, but the first peak appears to have grown in intensity relative to the second. This can be explained by the presence of the two CH_3 groups in methyl methanesulfonate. The transitions in methyl trifluoromethanesulfonate – to 3s/σ*(C-H) and 3p/σ*(C-H) orbitals of the O-CH_3 group – should also appear in methyl methanesulfonate. Because methyl methanesulfonate has an extra CH_3 group, the transition seen in sodium methanesulfonate – to 3p/σ*(C-H) of the S-CH_3 group – should also be seen. This means that the first peak in methyl methanesulfonate is caused by transitions to 3s/σ*$(C\text{-}H)_{C\text{-}O}$ and 3p/σ*$(C\text{-}H)_{C\text{-}S}$ orbitals where the subscript shows the immediate chemical environment of the carbon atom. Summing these two transitions explains the increased intensity of that first peak. The second peak is caused by a transition to a 3p/σ*$(C\text{-}H)_{C\text{-}O}$ orbital, just as in methyl trifluoromethanesulfonate.

In the spectra of DMSO and methanethiol, transitions at ~287 eV are to σ*(C-S) orbitals. The existence of this transition in the sulfonate spectra is supported by GSCF3 calculations on methanesulfonic acid, which show an orbital of σ*(C-S) character as well as one of σ*(C-H) character. As such, transitions to σ*(C-S) orbitals have been assigned, overlapping with the σ*(C-H) peaks. In methanol and propanol, a σ*(C-O) transition appears at ~293 eV.[29] The energy and appearance of this peak in alcohols matches well with the hump above the two CH_3 peaks seen in methyl methanesulfonate. A σ*(C-O) transition is also expected in methyl trifluoromethanesulfonate, and is probably hidden under the two σ*(CF_3)peaks. It is surprising that a similar peak shows up so clearly in sodium methanesulfonate, since this molecule does not have carbon-oxygen bonds, so another process might also contribute to this feature. Finally, the broad feature at 300-305 eV is assigned to a shape resonance, as in the spectra of C_2F_6 and DMSO. It is most visible in the spectra of the fluorinated molecules because of the larger centrifugal potential barrier caused by the electronegative fluorine atoms of the CF_3 group.[19,28]

The GSCF3 calculations on methanesulfonic acid show σ*(C-S) character for the first peak and σ*(C-H) character for the second, which agrees with the other sulfonate spectra, but in the experimental spectrum these peaks are clearly resolved, which is not the case for the other sulfonates. The third and fourth peaks in the experimental spectrum could not be identified, and the fifth is attributed to a shape resonance just as in the other molecules. The

exact reasons for the differences in the spectrum of the acid from the other molecules are uncertain, but suggest that the presence of an OH group even several bonds away influences the electronic environment of the carbon atom significantly.

3.2.2. Discussion of Important Results from the C 1s Edge

The carbon-based PTFE backbone has several features worth monitoring for their relationship to fuel cell performance. First, errors in the synthesis of PFSA that leave some CH bonds in the backbone, discussed briefly for the S 2p spectra, could impact membrane function.[5] Second, attack of PFSA by peroxy radicals is believed to cause the loss of CF_2 groups relative to sulfonate heads, since effluent water from the cathode area is usually fluorine-rich.[7,30] Although not tied to the backbone structure, this study also looked at the spectral changes brought on by methylating a sulfonate oxygens, which would prevent this oxygen from contributing to proton conduction.

The C 1s spectra of the molecules recorded here show trends with fluorination and methylation. The molecule that most closely resembles deprotonated PFSA is ammonium trifluoromethanesulfonate. The spectrum of this molecule gives only two peaks, both assigned to transitions in the CF_3 group. Methylation of the sulfonate oxygen adds two new peaks, related to transitions in the CH_3 group. Defluorinating eliminates the two CF_3 peaks but preserves the two CH_3 peaks, and finally, demethylating leaves only one CH_3 peak. By looking to this pattern of changes rather than aiming to make precise peak assignments, the C 1s edge can be used to easily identify certain modifications to PFSA.

Firstly, the relative ratios of CF_3 and CH_3 groups in the backbone can be checked, since the CF_3 and CH_3 peaks have been found to be so nicely resolved. It should be noted that the backbone of PFSA contains CF_2 groups as opposed to the CF_3 groups in these reference molecules. The effect on spectra of CF_3 rather than CF_2 groups has been studied by comparing perfluoro-*n*-alkanes (CF_3 and CF_2 groups) to perfluorocycloalkanes (CF_2 groups only), and it has been concluded that the spectral features of excitations in CF_2 groups are analogous to but at lower energy by ~2.3 eV than features of excitations in CF_3 groups.[28] Based on the spectra reported here, even if the peaks given by CF_2 carbon atoms were shifted by this much, they would still be distinct from peaks given by alkyl groups. Second, the C 1s edge gives a relatively simple way of checking if a methyl group has been attached to a

sulfonate oxygen. Counting the number of peaks below ~292 eV should give an indication of whether the oxygen is naked or bonded to some non-carbon species (one peak), or methylated (two peaks). Finally, a reduction in the intensity of peaks assigned to fluorinated carbons in STXM spectra can show that loss of CF_2 groups – and therefore degradation by peroxy radicals – has occurred because of cell use.

3.3. Oxygen 1s Edge

3.3.1. Peak Assignments

The O 1s spectra of the five sulfonates studied are shown in **Figure 13**, and **Table 3** gives peak energies and assignments. The spectra of the sulfonate salts and sulfonic acid esters show one broad peak with several shoulders at ~536-538 eV. In DMSO, the main transition responsible for a similar broad peak at 532.66 eV is to a σ*(S-O) orbital, so the main peak in the spectra of the sulfonates has been assigned to this orbital.[19] This assignment is supported by the GSCF3 calculations on methanesulfonic acid. For the double-bonded oxygens, excitations are almost exclusively to molecular orbitals with σ*(S-O) character.

The width of the first peak suggests that transitions to orbitals with character other than σ*(S-O) contribute some intensity. A σ*(C-O) peak shows up in propanol at 537.2 eV, in methanol at 537.3 eV and in methyl formate at 536.9 eV, so it seems likely that an O 1s→σ*(C-O) transition is present in the sulfonic acid ester spectra and contributes to the main peak.[29,31] By comparison with shoulders in the DMSO O 1s spectrum, the remaining shoulders on the sulfonate main peak have been assigned to transitions to O s and d Rydberg orbitals, and the highest-energy humps to 3d shape resonances.

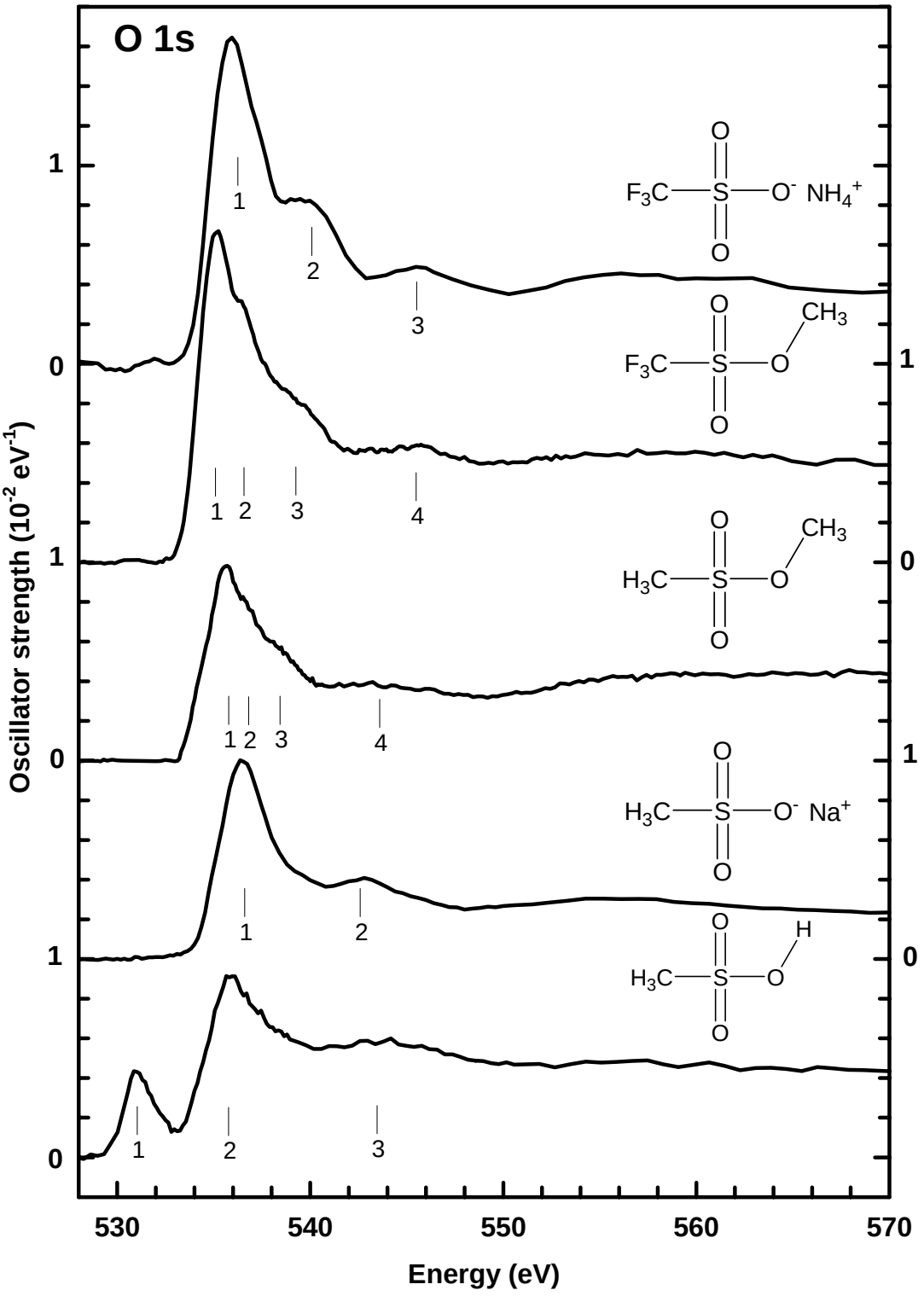

Figure 13. O 1s spectra of the species recorded.

Molecule	Feature	Energy loss (eV)	Assignment (from O 1s)
Ammonium trifluoromethanesulfonate	1 2 3	535.93 539.47 545.61	σ*(S-O) s and d Rydbergs 3d shape resonance
Methyl trifluoromethanesulfonate	1 2 3 4	535.20 536.40 538.94 545.62	σ*(S-O), σ*(C-O) s and d Rydbergs s and d Rydbergs 3d shape resonance
Methyl methanesulfonate	1 2 3 4	535.60 536.64 538.11 543.28	σ*(S-O), σ*(C-O) s and d Rydbergs s and d Rydbergs 3d shape resonance
Sodium methanesulfonate	1 2	536.40 542.83	σ*(S-O) 3d shape resonance
Methanesulfonic acid	1 2 3	531.0 535.92 543.58	σ*(O-H) σ*(S-O) 3d shape resonance

Table 3. Peak energies and assignments for the O 1s spectra of the species recorded.

The O 1s spectrum of methanesulfonic acid shows a distinct feature well below the main O 1s peak of the other species, at 531 eV. This peak is not seen in the spectra any of the other literature sulfur species referred to here, but a comparable peak does show up in the spectra of alcohols. Both propanol and methanol have a peak at ~534 eV, which is below the other O 1s features of these molecules.[29] This peak is assigned, in both cases, to a transition to a σ*(O-H) orbital. Applying this assignment to methanesulfonic acid makes sense, since this transition would be expected only in the acid and not in the esters or salts. GSCF3 calculations do indeed show an orbital of σ*(O-H) character, shown in **Figure 14**.

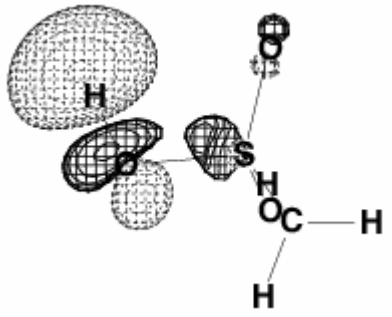

Figure 14. σ*(O-H) orbital predicted in methanesulfonic acid by GSCF3 calculations.

Oddly, the results of GSCF3 calculations place the orbital of σ*(O-H) character at higher energy than the σ*(S-O) orbital. Since this leads to assignments that do not agree with the spectra of alcohols or of the other sulfonates, the accuracy of the GSCF3 calculations at this edge is doubted, and the 531 eV peak in methanesulfonic acid has been assigned to a σ*(O-H) orbital. It would be helpful to repeat the calculations perhaps with a different basis set and certainly on other sulfonate molecules, to see if a similar energy switch is observed.

3.3.2. Discussion of Important Results from the O 1s Edge

In PEM fuel cells, PFSA polymers are crucial for proton conduction. When the membrane is sufficiently hydrated, protons can hop between PFSA R-SO_3^- groups and H_2O molecules, travelling through the membrane.[5] If protonated sulfonic acids could be distinguished spectroscopically from anionic sulfonates and sulfonates bonded to some non-hydrogen species, STXM could be used as a spatially-resolved probe to follow proton transfer. For this reason, it is important to identify spectral features that give some indication of the group or charge on the sulfonate oxygens.

The spectra of the sulfonic acid esters and sulfonate salts are quite similar. Distinguishing between these species seems best left to the C 1s edge. The spectrum of methanesulfonic acid, on the other hand, is easily distinguished by its 531 eV peak, assigned to a σ*(O-H) transition as discussed above. If this assignment is correct, then this peak would be expected only in the spectrum of protonated PFSA. Because it is so well-resolved from the main O 1s peak of the other sulfonates, it has the potential to act as the fingerprinting tool needed to follow proton transfer in the PEM spectroscopically.

Comparison of the O 1s spectra also leads to a conclusion that is perhaps less pertinent to fuel cells but of interest in a different way. If the structure of the sulfonate groups is as shown in **Figure 15a**, which is the one most commonly used in textbooks, then transitions to π*(S=O) and σ*(S-O) orbitals should occur, and these transitions would be expected at distinguishable energies. This is the case in carboxylic acids.[31] In propanoic acid, for example, excitations to π*(C=O) from O 1s(C=O) and O 1s(OH) appear at 532.1 and 535.4 eV respectively, while excitations to σ*(C-O) from the same O 1s orbitals are at 540.2 eV and 543 eV respectively.[31] Instead, the S 2p spectra reported here show only one peak,

assigned to a σ*(S-O) orbital. This is what would be expected if the sulfonate Lewis structure was more accurately depicted by **Figure 15b.**

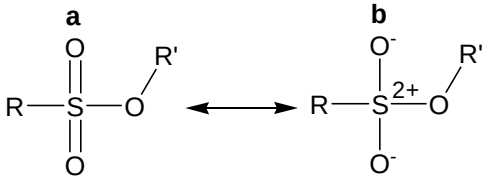

Figure 15. Possible Lewis structures of sulfonates, with **a)** double bonds, and **b)** single bonds only.

GSCF3 calculations on methanesulfonic acid also support this view of the S-O bond. **Figure 16** displays the orbitals that contribute most strongly to the O 1s spectra of the formally double-bonded oxygens. The orbitals are primarily of σ*(S-O) character. Even when they show the possibility for side-on π-style interaction, as in orbital **c**, it is clear that the extent of the side-on overlap of S and O atomic orbitals is smaller than the head-on overlap.

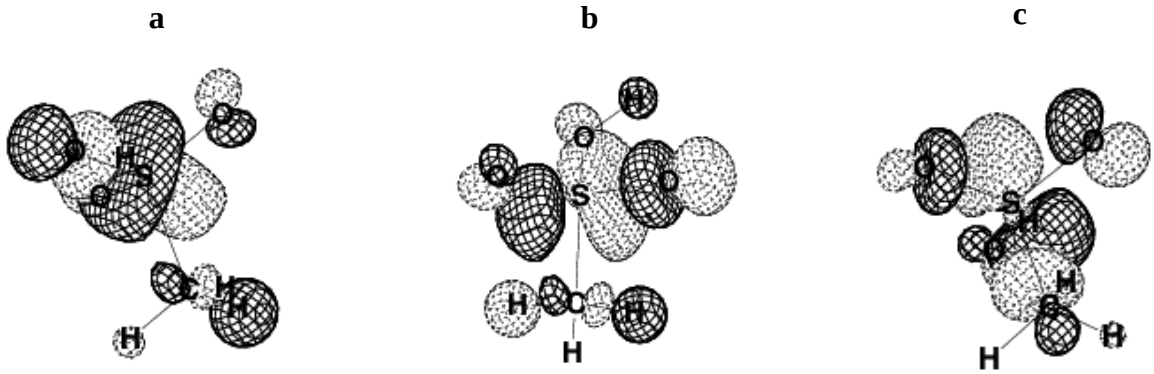

Figure 16. GSCF3-calculated orbitals to which excitation from one of the formally double-bonded oxygens takes place, showing mainly σ*(S-O) character.

This is certainly not the first suggestion that the second Lewis structure might better describe the sulfur-oxygen bond in these and other related molecules. Gilbert Lewis himself first used a similar structure when describing the bonding in sulfates, and it was only many years later that Linus Pauling proposed the involvement of the sulfur 3d orbitals in π bonding with oxygen 2p orbitals to give the structure found commonly in textbooks today.[32,33] Since then, many levels of calculation have been applied to gain insight into the nature of the sulfur-oxygen bond, and although it is generally accepted that the S $3d_{x2-y2}$ and d_{z2} orbitals on

sulfur can π bond with oxygen, the extent to which these orbitals contribute to bonding in sulfonates and related species is still open to debate. [34-36] By providing experimental support for the theory that the double-bond character is minimal, the O 1s spectra show the contribution to fundamental questions of bonding that ISEELS can make.

3.4. Fluorine 1s Edge

3.4.1. Peak Assignments

The F 1s spectra of the fluorinated molecules studied are shown in **Figure 17**, and **Table 4** gives peak energies and assignments. A broad peak appears in these spectra. The width of this peak is typical of F 1s spectra, and is caused by the dissociative nature of the ground state produced upon excitation of an electron to a higher state.[28]

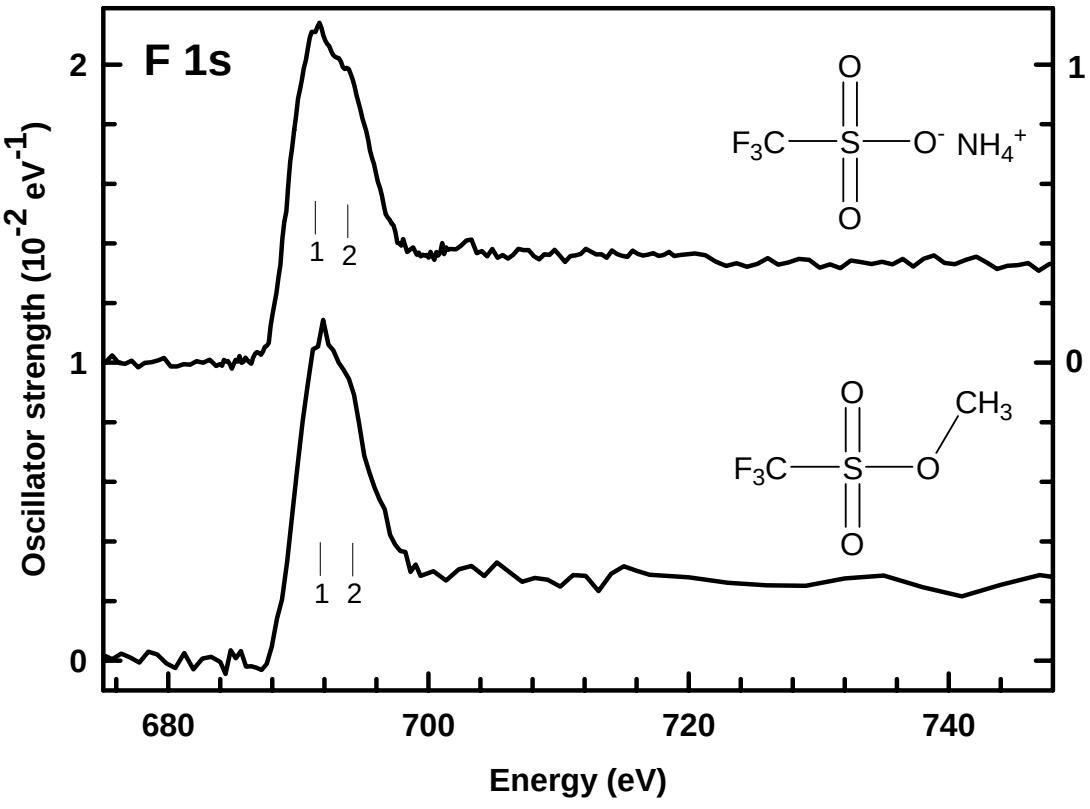

Figure 17. F 1s spectra of the fluorinated species recorded.

In the spectra of perfluorinated alkanes, it has been noted that transitions from F 1s and C 1s cores usually terminate in the same orbital.[28] Thus the F 1s spectra of the sulfonates are expected to show transitions to the $\sigma^*(C\text{-}F)_e$ and $\sigma^*(C\text{-}F)_{a1}$ orbitals that also contribute to the C 1s spectra. Indeed, these transitions have been identified in the spectrum of C_2F_6. In that spectrum they are spaced 2.7 eV apart, which agrees fairly well with the 2.1 eV spacing of the features assigned to these transition in the spectra reported here.

Molecule	Feature	Energy loss (eV)	Assignment (from F 1s)
Ammonium trifluoromethanesulfonate	1 2	691.92 693.85	$\sigma^*(C\text{-}F)_e$ $\sigma^*(C\text{-}F)_{a1}$
Methyl trifluoromethanesulfonate	1 2	691.60 693.71	$\sigma^*(C\text{-}F)_e$ $\sigma^*(C\text{-}F)_{a1}$

Table 4. Peak energies and assignments for the F 1s spectra of the species recorded.

3.4.2. Discussion of Important Results from the F 1s Edge

As described for other edges, the loss of fluorine from PFSA is an indication of degradation of the PFSA backbone caused by peroxy radicals.[30] Because of this, quantifying the amount of fluorine in an MEA before and after use could show whether peroxy radicals are active in the PEM.

The F 1s spectra reported here are nearly identical, proving that differences that are a few bonds away from the PTFE chain of PFSA will have no impact on the F 1s edge. This observation shows that although the F 1s edge cannot identify changes in the sulfonate heads of PFSA, it is ideal for quantifying the amount of fluorinated PTFE backbone in a region of the PEM. Because differences in spectral features imposed by modifications to the sulfonate groups do not have to be taken into account, the intensity of the broad F 1s peak gives a measure of the amount of PTFE backbone in a region, regardless of the sulfonate group to which that backbone is attached. This gives us a way of efficiently quantifying backbone distribution by looking only to a narrow range of energies.

3.5. STXM-ISEELS Comparison

When ISEELS was first built, the spectra it produced were of far superior quality to the ones that could be recorded at synchrotron radiation facilities. In the past several decades, huge advancements in synchrotrons have been made, so this is no longer the case. In fact,

when using ISEELS today one is often faced by the question of whether synchrotron facilities have made ISEELS obsolete. The use of both ISEELS and synchrotron-based STXM in this project provides a perspective on this question.

In order to compare the optimal spectra that STXM and ISEELS can give, the C 1s spectrum of CO_2 was measured on both instruments. A comparison is shown in **Figure 18**. The STXM spectrum is clearly of higher quality than the ISEELS spectrum. The resolution is better on STXM, as evidenced by the narrower full width at half-maximum (FWHM). This allows a peak at 296.3 eV, corresponding to the C 1s→4p transition, to be seen in the STXM spectrum but not appear at all when ISEELS is used.

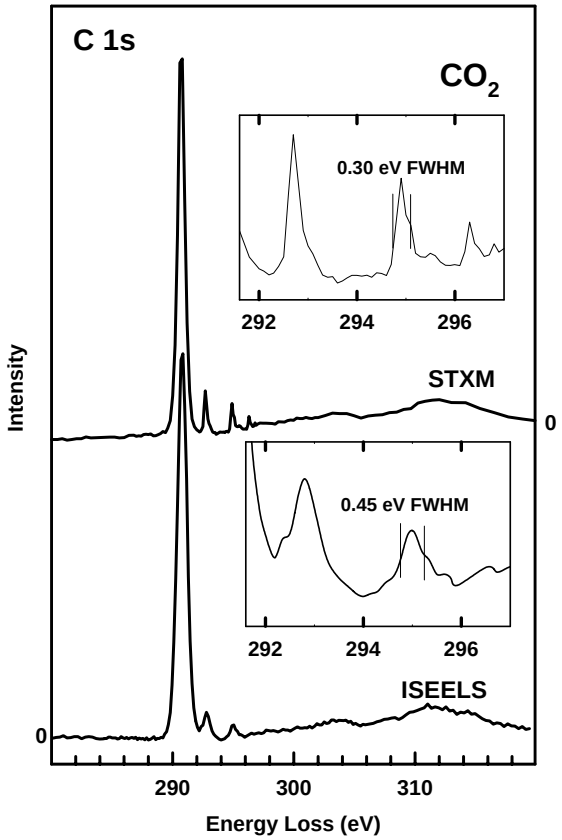

Figure 18. CO_2 C 1s spectra recorded on STXM and ISEELS.

To see if a similar difference would be seen in spectra of the sulfur reference compounds, a sample of methyl trifluoromethanesulfonate was run on STXM and ISEELS. In these spectra, shown in **Figure 19**, the better resolution of STXM is lost and the ISEELS

spectrum is of higher quality. The reproducibility of the spectra on STXM was also poor, with samples prepared at different times and in slightly different ways giving spectra that varied widely in quality. Finally, a peak in the STXM spectrum at ~285 eV indicates an impurity, which is likely the epoxy used in sample preparation. This reversal in performance can be largely attributed to differences in the way sample is introduced to STXM and ISEELS. STXM requires sample preparation that can give samples that are too thick or too thin and introduce impurities. In ISEELS, a compound is essentially distilled into the spectrometer and the pressure can be adjusted with leak valves until the amount of sample in the spectrometer is just right. This is certainly not to say that every molecule is easily run on ISEELS. In this project, several weeks were spent trying to record spectra of triflic acid, which was eventually abandoned because it reacted so strongly with everything it touched including the inside of the spectrometer. However, this experience confirms that ISEELS has a lot of advantages, especially as a means of acquiring reference spectra of pure compounds.

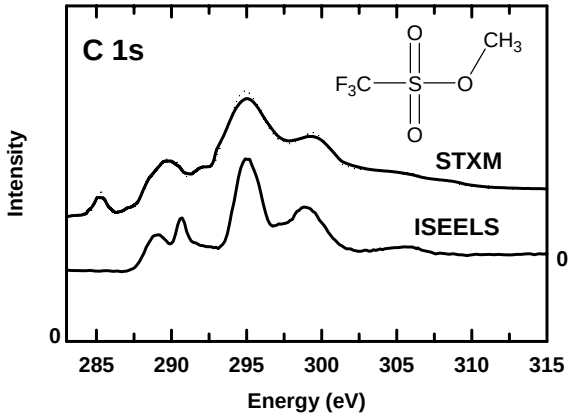

Figure 19. Methyl trifluoromethanesulfonate C 1s spectra recorded on STXM and ISEELS.

4. Conclusions and Suggestions for Further Research

Based on the five sulfonate species studied here, it seems that using reference spectra to interpret STXM spectra could help significantly with the characterization of changes to PFSA in fuel cells. The spectra of methyl methanesulfonate, methyl trifluoromethanesulfonate, methanesulfonic acid, ammonium trifluoromethanesulfonate and sodium methanesulfonate reflect differences in chemical structure of the sort that are

expected in PFSA over a fuel cell's lifetime. Moreover, they point to the fact that STXM can be used most efficiently by tailoring the spectra recorded to the aspect of fuel cell materials under investigation. Thus the S 2p edge should be used to check sulfur oxidation state, the C 1s edge to monitor backbone fluorination and sulfonate methylation, the O 1s edge to follow proton conduction and the F 1s edge to quantify PFSA backbone distribution.

These results suggest ways to accurately and efficiently learn about what goes on inside a fuel cell, but there is certainly room for more work. For one, many molecules with important roles in fuel cells have analogues outside of the sulfonate family. Even PFSA has features that may be best simulated by different reference species, since its PTFE backbone is linked by oxygens to give an ether-like structure. A future study could characterize simple ether analogues of the PFSA backbone, to gain further insight into spectral features of PFSA structural changes. Developing on this project could also lead in new directions. One goal could be to study the kinetics of proton transfer in membranes. Such a study would be complemented by electrochemistry and NMR, but being able to identify protonated PFSA spectroscopically would be crucial to its success, and this project has taken steps toward making that possible.

Acknowledgements

Thank you to Dr. Hitchcock for his guidance during this 4G09 project. Thank you also to the Hitchcock lab group for their support, and to the Goward, Brook and Emslie groups for lending some materials and liquid nitrogen to this project.

References

1. Wolfson, S.K.; Yao, S.J.; Geisel, A.; Cash, H.R. *ASAIO J.* **1970**, *16*, 193.

2. Adlhart, O.J. Fuel cell system utilizing ion exchange membranes and bipolar plates. US Patent 4175165A, July 20, 1977.

3. El-kharouf, A.; Chandan, A.; Hattenberger, M; Pollet, B.G. *J. En. Inst.* **2012**,*85*, 188.

4. Yu, Y.; Li, H.; Wang, H.; Yuan, X-Z.; Wang, G.; Pan, M. *J. Power Sources* **2012**, *205*,

5. Rama, P.; Chen, R.; Andrews, J. *Proc. IMechE.* **2008**, *222*, 421

6. Debe, M. K. *Nature* **2012**, *486*, 43.

7. Bessarabov, D.; Hitchcock, A. *Membrane Technology* **2009**, *12*, 6.

8. Zhang, S.; Yuan, X-Z.; Cheng, J.N.; Haijiang, W.; Wu, J.; Friedrich K.A.; Schulze, M. *J. Power Sources* **2010**, *195*, 1142.

9. Kundu, S.; Cimenti, M.; Lee, S.; Bessarabov, D. *Membrane Technology* **2009**, *10*, 7.

10. Wu, J.; Yuan, X-Z.; Martin, J.J.; Wang, H.; Yang, D.; Qiao, J.; Ma, J. *J. Power Sources* **2010**, *195*, 1171.

11. Yu, J.; Jian, Z.; Hou, M.; Liang, D.; Xiao, Y.; Dou, M.; Shao, Z.; Yi, B. *J. Power Sources* **2014**, *246*, 90.

12. Hitchcock, A. P. *J. Electron Spectrosc.* **2000**, *112*, 9.

13. Brion, C. E.; Daviel, S.; Sodhi, R. N. S.; Hitchcock, A. P. *AIP Conf. Proc*. **1982**, *94*, 429.

14. Sodhi, R. N. S.; Brion, C. E. *J. Electron Spectrosc. Relat. Phenom*. **1984**, *34*, 363.

15. Kosugi, N.; Kuroda, H. *Chem. Phys. Lett.* **1980**, *74*, 490

16. Huzinaga, S.; Andzelm, J.; Klobokowski, M.; Radzio-Andzelm, E.; Sasaki, Y.; Tatewaki, H. *Gaussian Basis Sets for Molecular Calculations*; Elsevier: Amsterdam, 1984.

17. Sze, K.H.; Brion, C.E.; Tong, X-M.; Li, J-M. *Chem. Phys.* **1987**, *115*, 433.

18. Ferrett, T. A.; Heimann, P.A.; Kerkhoff, H.G.; Becker, U.; Lindle, D.W; Shirley, D.A. *Chem. Phys. Lett.* **1987**, *138*, 607.

19. Sze, K. H.; Brion, C.E.; Tronc, M.; Brodeur, S.; Hitchcock, S. *Chem. Phys.* **1988**, *121*, 279.

20. Dezarnaud, C.; Tronc, M.; Hitchcock, A. P. *Chem. Phys.* **1990**, *142*, 455.

21. Hitchcock, A. P.; Horsley, J. A.; Stohr, J. *J. Chem. Phys.* **1986**, *85*, 4835.

22. Mulliken, R. S. *J. Am. Chem. Soc.* **1964**, *86*, 3183.

23. Jurgenson, A.; Kosugi, N.; Cavell, R.G. *Chem. Phys.* **1999**, *247*, 445

24. Cooney, R. R.; Urquhart, S. G. *J. Phys. Chem. B.* **2004**, *108*, 18185.

25. Yates, B.W.; Shinozaki, D.M.; Kumar, Z.A.; Meath, W.J. *J. Polym. Sci. Pol. Phys.* **1993**, *31*, 1837.

26. Dehmer, J.L.; Dill, D.; Wallace, S. *Phys. Rev. Lett.* **1979**, *43*, 1005.

27. Hay, S. J.; Metson, J. B.; Hyland, M. M. *Ind. Eng. Res. Chem.* **2004**, *43*, 1690.

28. Ishii, I.; McLaren, R.; Hitchcock, A.P.; Jordan, K.D.; Choi, Y.; Robin, M.B. *Can. J. Chem.* **1988**, *66*, 2104.

29. Ishii, I.; Hitchcock, A. P. *J. Elec. Spec.* **1988**, *46*, 55.

30. Tang, H; Peikang, S.; Jiang, S.P.; Wang, F.; Pan, M. *J. Power Sources* **2007**, *170*, 85.

31. Ishii, I.; Hitchcock, A. P. *J. Chem. Phys.* **1987**, *87*, 830.

32. Lewis, G.N. *J. Am. Chem. Soc.* **1916**, *38*, 762.

33. Pauling, L. *J. Phys. Chem.* **1952**, *56*, 361.

34. Cruickshank, D.W.J. *J. Chem. Soc.* **1961**, 5486.

35. Stefan, T.; Janoschek, R. *J. Mol. Model.* **2000**, *6*, 282.

36. Moffitt, W. *Proc. R. Soc. Lond.* **1950**, *200*, 409.

Appendix 1: Methanesulfonic acid mass spectrum.

Compound Mass Spectrum Report - MS

File Name: SF140401B.D **Instrument:** Instrumen **Print Date:** 4/1/2014 4:54:15 PM
Method: SLWFSSPLIT100B **Operator:** SF **Acq. Date:** 4/1/2014 12:12:00 PM
Sample Name: Methanesulfonic acid
Analysis Info: 24333

Acquisition Parameter:

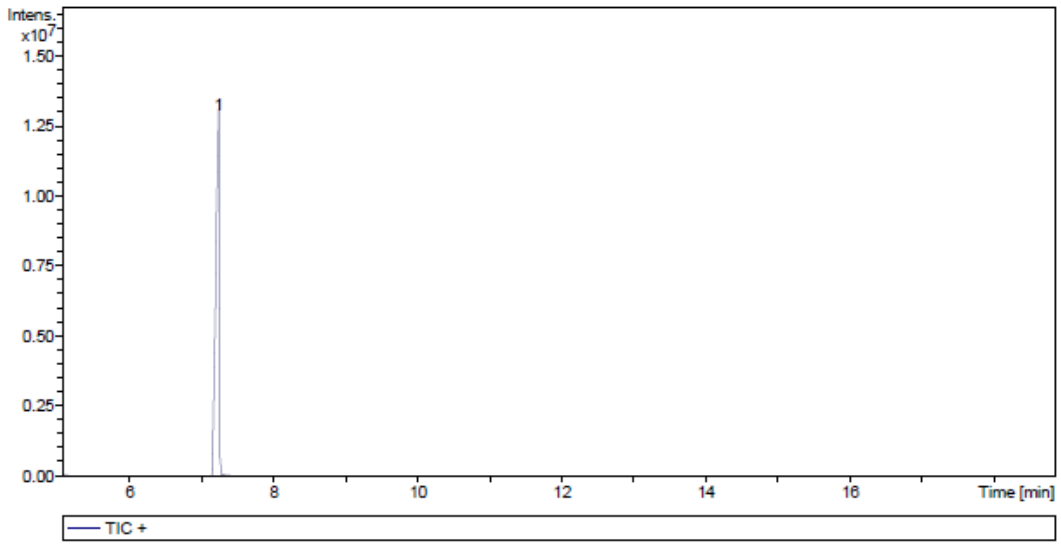

Compound List:

#	RT [min]	Range [min]	Height	Area	Area Frac. %
1	7.2	7.1 - 7.4	12907406	46478742	100.0

Cmpd 1, 7.2 min

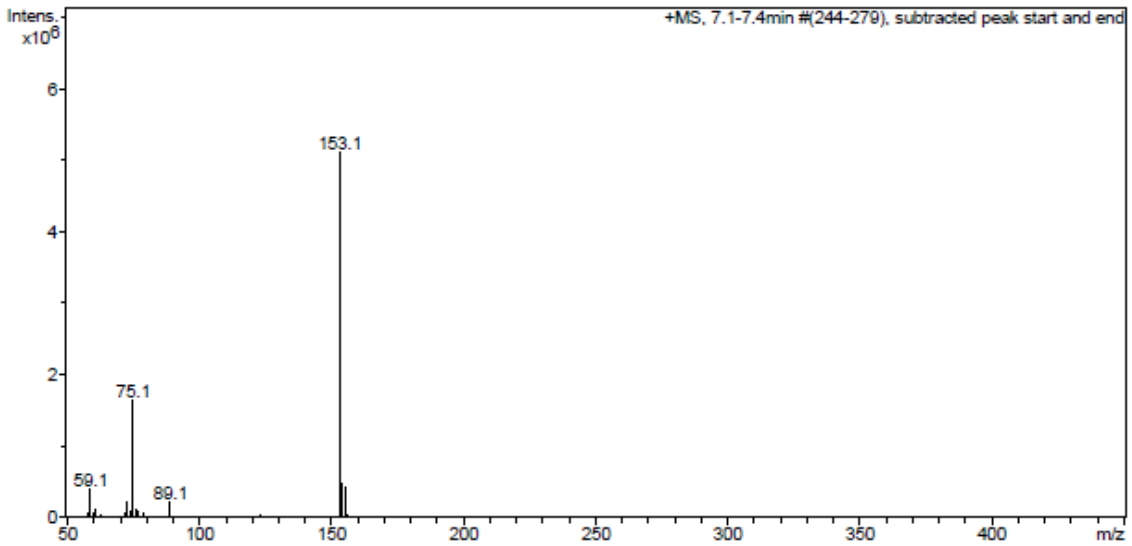

Appendix 2: STXM OD1 spectra

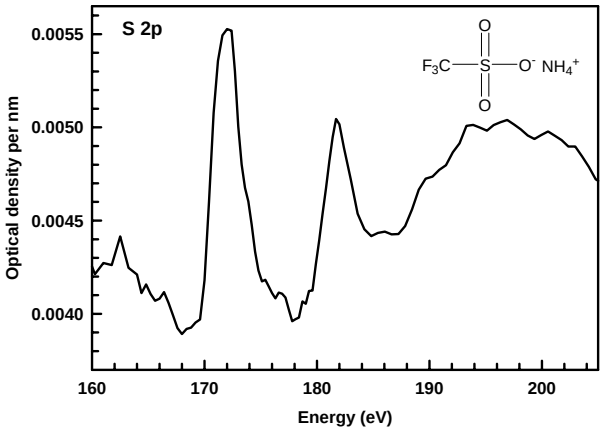

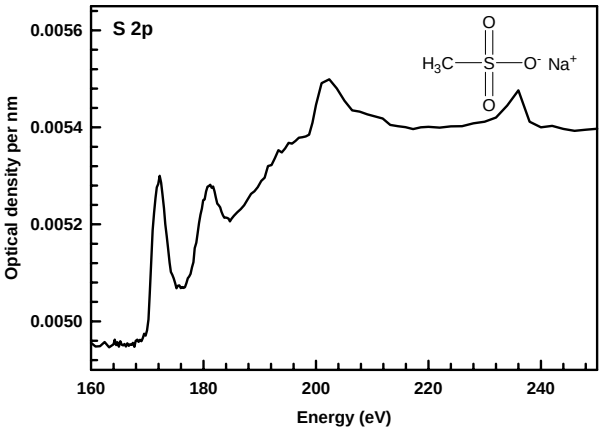

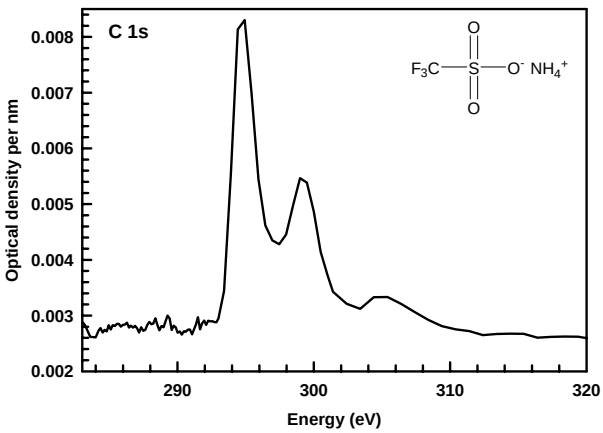

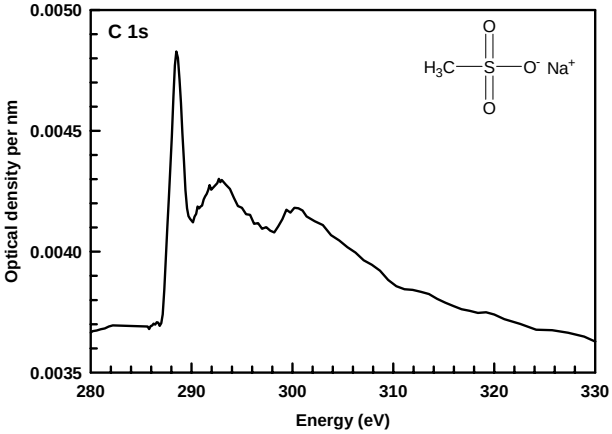

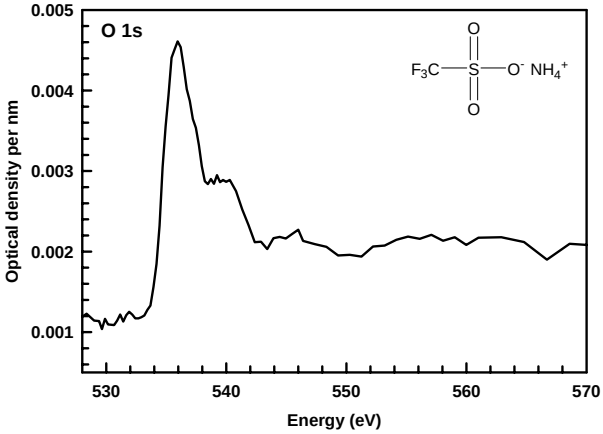

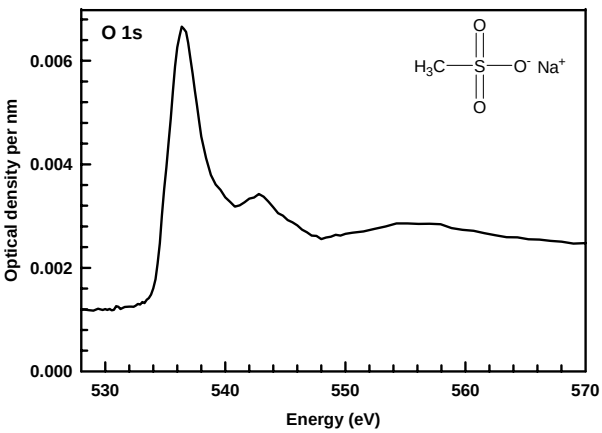

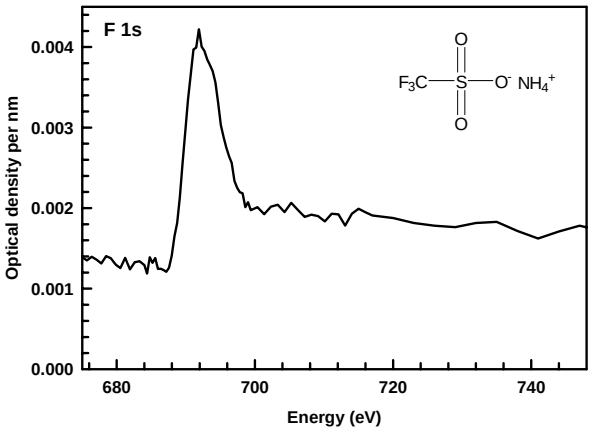
F 1s
Optical density per nm
0.000
0.001
0.002
0.003
0.004
680
700
720
740
Energy (eV)
O
F3C—S—O- NH4+
O

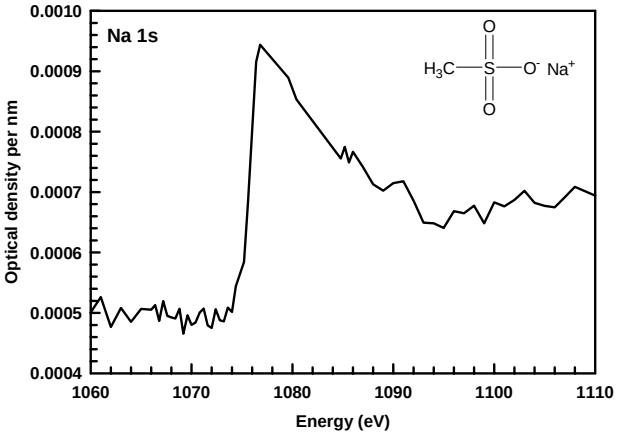
Na 1s
Optical density per nm
0.0004
0.0005
0.0006
0.0007
0.0008
0.0009
0.0010
1060
1070
1080
1090
1100
1110
Energy (eV)
O
H3C—S—O- Na+
O

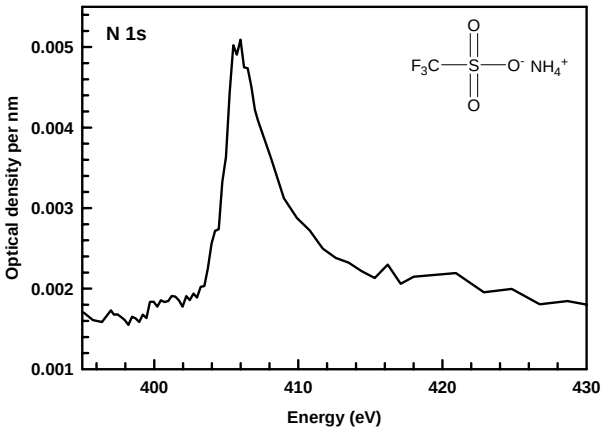
N 1s
Optical density per nm
0.001
0.002
0.003
0.004
0.005
400
410
420
430
Energy (eV)
O
F3C—S—O- NH4+
O

Appendix 3: GSCF3 calculations for methanesulfonic acid

Atom	x coordinate	y coordinate	z coordinate
O1	0.1859	0.379	-1.5682
S	0.3081	0.648	-0.0066
O2	1.6934	0.528	0.3162
O3	-0.4086	1.834	0.3047
C	-0.5804	-0.736	0.6274
H1	1.0588	0.345	-1.9526
H2	-0.0789	-1.645	0.3293
H3	-1.5904	-0.707	0.2451
H4	-0.5879	-0.644	1.7047

Table 1: Coordinates of methanesulfonic acid atoms, calculated by Spartan at the 6-31G* level. The figure below shows the numbering scheme used.

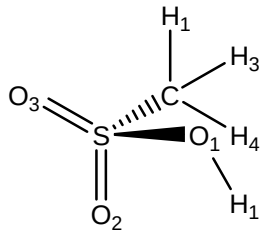

Figure 1. Numbering scheme used for atoms in methanesulfonic acid GSCF3 input.

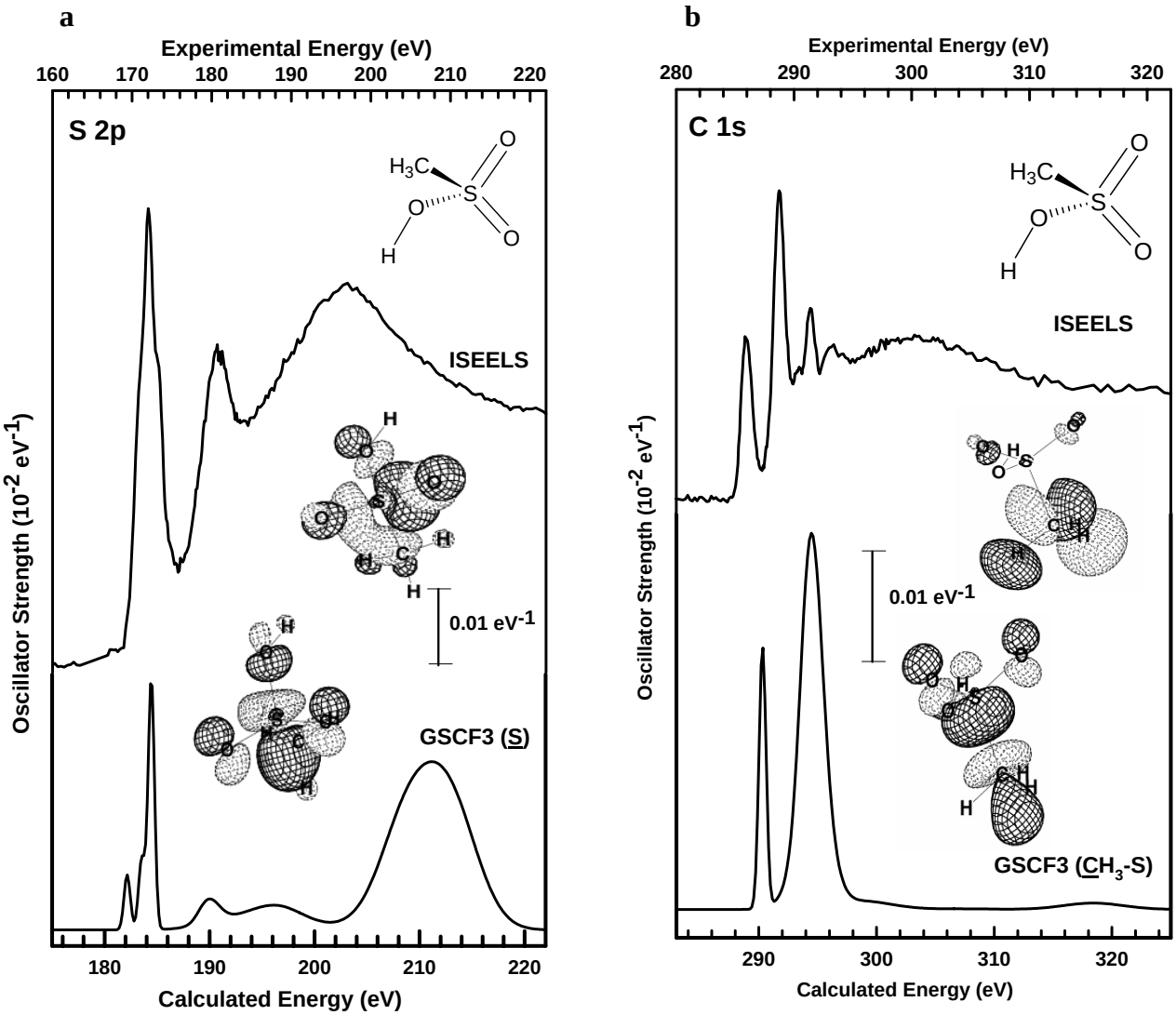
a
Experimental Energy (eV)
160 170 180 190 200 210 220
S 2p
ISEELS
0.01 eV-1
GSCF3 (S)
Oscillator Strength (10-2 eV-1)
180 190 200 210 220
Calculated Energy (eV)
b
Experimental Energy (eV)
280 290 300 310 320
C 1s
ISEELS
0.01 eV-1
GSCF3 (CH3-S)
Oscillator Strength (10-2 eV-1)
290 300 310 320
Calculated Energy (eV)

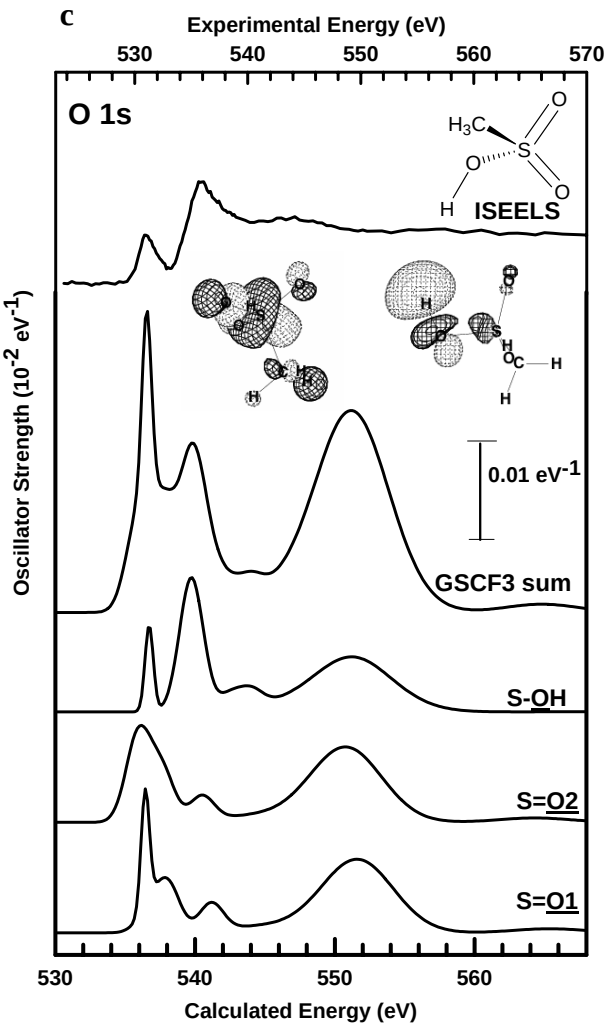

Figure 2. Calculated and experimental spectra of methanesulfonic acid at the **a)** S 2p, **b)** C 1s and **c)** O 1s edge. Note that rigid energy shifts of the calculated spectra by 7 eV for O 1s, 3 eV for C 1s, 15 eV for S 2p have been incorporated into the plots, for ease of comparison of the calculated and experimental spectra. Virtual orbitals to which excitations correspond are also shown in the plots.

Site	IP (eV)	Assignment	ε (eV)	*f* (10^{-2})
S[a]	186.878	Rydberg	-0.173	0.51
		Rydberg	-0.124	0.61
		Rydberg	-0.089	0.02
		Rydberg	0.105	0.52
C[b]	292.867	σ*(C-S)	-0.094	1.39
		σ*(C-H)	0.047	2.44
O (S=O2)[c]	538.475	σ*(S-O)	-0.075	0.78
		σ*/π*(S-O)	-0.015	0.91
		σ*(S-O)	0.099	0.53
O (S=O3)[c]	537.754	σ*(S-O)	-0.072	1.21
		σ*/π*(S-O)	-0.002	0.93
		σ*(S-O)	0.101	0.47
O (S-OH)[c]	540.099	σ*(S-O)	-0.124	0.59
		σ*(O-H)	-0.013	2.54

Table 2. Calculated ionization potentials (IP) and peak energies, intensities (*f*) and assignments for each atom in methanesulfonic acid.

a) Basis functions (Huzinaga *et al.*)[16]: No core hole: HTS0X (333 33). If given the core hole: HTS3X (533 53).
b) Basis functions[16]: No core hole: HTS4X (53 4). If given the core hole: HTS6X (41121 2111).
c) Basis functions[16]: No core hole: HTS4X (53 4). If given the core hole: HTS6X (41121 2111).